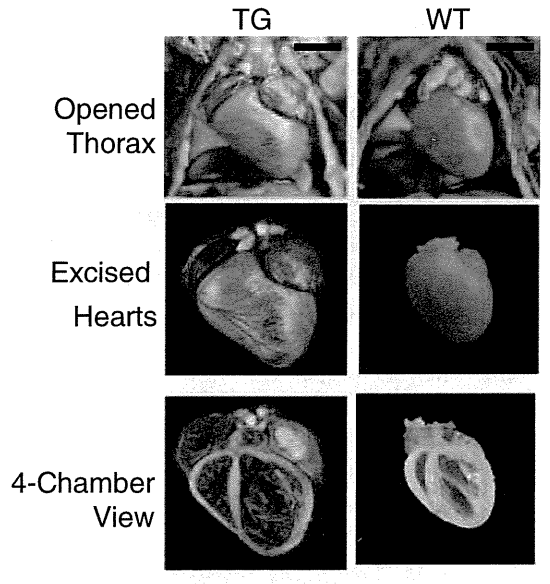

Fig. 3. The hearts of 6-month-old transgenic (TG) mice homozygous for the ST3Gal-II transgene were much larger than those of wild-type (WT) mice. TG heart shows severe dilatation of all four chambers with thin, low tensile-strength walls. Bars = 5 mm.

in the ganglioside composition in the heart, brain, or liver between the TG and WT mice (Fig. 5).

Lectin blot analysis of heart proteins. Alterations in the sugar moieties of heart glycoproteins were examined by lectin blot staining in two fractions of heart proteins from 10-week-old mice (Fig. 6A, 6B). Three lectins were used: *Maackia amurensis* seed lectins (MAA) recognize α2,3-sialylation of sugars, such as Gal-GalNAc; peanut lectins (PNA) recognize non-sialylated Gal-GalNAc sugars; concanavalin A (ConA) recognizes high-mannose-type sugars. Staining with MAA and PNA lectins indicated that heart proteins of TG mice were less sialylated than those of WT mice, even though ST3Gal-II was overexpressed in the TG mice. One differentially stained ConA band was found in fraction 1 (soluble proteins containing cytosolic proteins), indicating that some cytosolic heart proteins in TG mice lost their high-mannose-type glycosylation, which was present in those of WT mice.

Calreticulin and calnexin expression in hearts. Quantitative Western blots with TG and

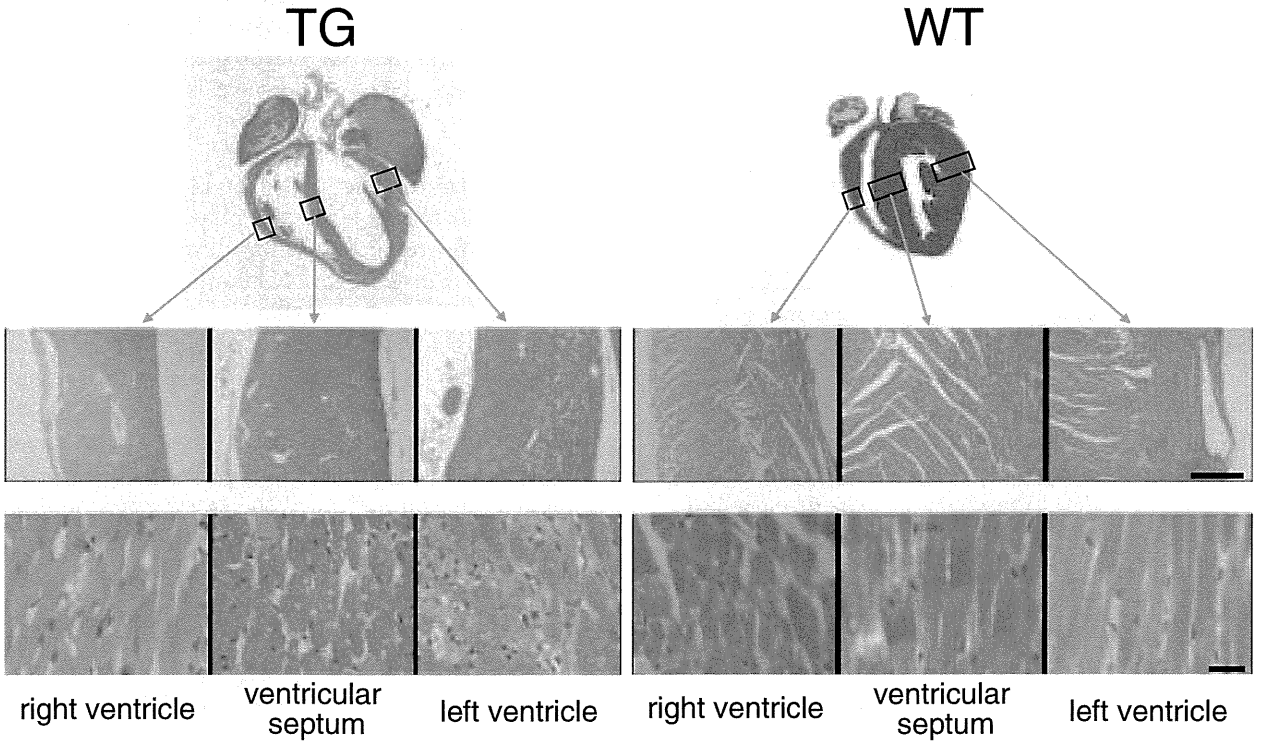

Fig. 4. Histopathological observations of hearts in 6-month-old transgenic (TG) and wild-type (WT) mice. Hematoxylin and eosin-stained tissue sections from three cavity walls, the positions of which are indicated by rectangles in the upper images and are shown in low (middle images, bar = 100 µm) and high (lower images, bar = 10 µm) magnifications. Slight fibrosis was observed sporadically in TG hearts, but no apparent cell infiltration was found in either TG or WT hearts.

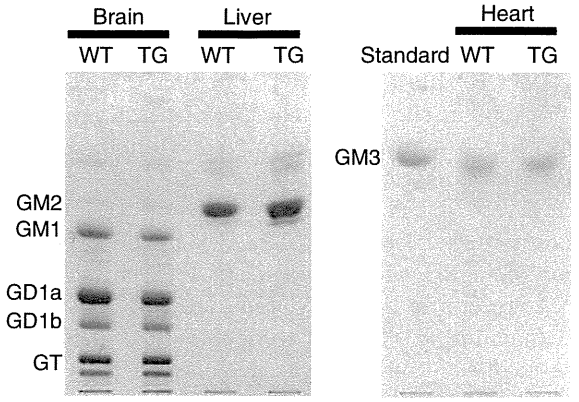

Fig. 5. Ganglioside analysis in the brain, liver, and heart. No difference in ganglioside composition was found in the brain, liver, or heart between 6-month-old transgenic (TG) and wild-type (WT) mice, as analyzed by thin-layer chromatography and resorcinol staining. The amounts of gangliosides per lane were equivalent to 1.5 mg, 5 mg, and 5 mg dry weight of the brain, liver and heart, respectively.

WT heart proteins at 10 weeks of age revealed a significant increase ($p < 0.05$) in the amounts of calreticulin and calnexin in the TG heart (Fig. 6C, 6D).

Lectin staining of heart and skeletal muscle tissues. Sialylation in heart and skeletal muscle tissues with transgene-derived ST3Gal-II was examined by histochemical analysis using PNA lectin in combination with α2,3-sialidase treatment (Fig. 7). The ST3Gal-II enzyme converts sugars (Galβ1,3GalNAc) that are bound by PNA to sugars (SialGalβ1, 3GalNAc) that are not bound by PNA by α2,3-sialylation of terminal galactose residues. The α2,3-sialidase enzyme reverses the reaction. In the heart, the staining was essentially the same between TG and WT mice with and without α2,3-sialidase treatment. In contrast, PNA staining in the TG skeletal muscle tissue was more intense than that in the WT tissue even without α2,3-sialidase treatment. Staining in skeletal muscle tissue was essentially the same between TG and WT mice after the α2,3-sialidase treatment. These results indicated that most of the terminal Galβ1,3GalNAc structures in pericellular regions (cell membranes and ECM) were sialylated *via* the α2,3 linkage of galactose residues in the heart. The sialylation decreased in skeletal muscle of TG mice compared with that in WT mice. After α2,3-sialidase treatment, the TG and WT tissues showed similar staining patterns, indicating that the differential staining by PNA without α2,3-sialidase treatment was attributable to differential α2,3-sialylation of Gal-GalNAc structures and not different amounts of Gal-GalNAc structures.

Discussion

The mice that were homozygous for the ST3Gal-II transgene developed non-inflammatory cardiac dilatation with relatively late onset and 100% lethality. Our findings suggest a new concept that abnormal glycosylation of heart proteins can cause cardiac dilatation *via* perturbation of ER/SR environments. Thus, the mice may be a new model for examining the mechanism and developing therapeutics of non-inflammatory cardiac dilatation related to abnormal glycosylation.

The severity and onset of cardiac symptoms in 4C30 mice depended on a level of transgene expression. As a 1-year observation revealed that cardiac dilatation in 4C30 mice was homozygous-specific, we first considered two issues with regard to the possible mechanism of the cardiac dilatation: the effect of genome disruption by transgene insertion and the effect of transgene dosage. However, after longer observation and chromosomal mapping of the transgene, we concluded that the effect of the transgene itself was the primary cause for two reasons. First, some hemizygous transgenic mice older than 18 months, about three times older than the homozygous transgenic mice, also showed mild cardiac symptoms, suggesting that a level of transgene expression, about one third in the hemizygous compared to that in the homozygous (Fig. 1C), may be involved in the severity and onset of symptoms. Second, our previous report on chromosomal mapping of the transgene in 4C30 mice by genomic walking[14] indicated that the transgenes were inserted into the B1.2 region of chromosome 11, approximately 200 kb upstream of the δ-sarcoglycan gene (Fig. 1E), an area in which no gene has been reported to date. Decreased δ-sarcoglycan expression was expected in homozygous mice because δ-sarcoglycan is a key component of the sarcomere complex in muscle tissues and its deficiency can cause degenerative heart diseases, including dilated cardiomyopathy.[18] However, δ-sarcoglycan was equally expressed in TG and WT mice (Figs. 1F and 1G), suggesting that the transgene insertion had no adverse effect on genes near the insertion site in TG mice.

The histological analysis indicated that TG mice have cardiac dilatation with a non-inflammatory mechanism. The causes of cardiac dilatation in humans, such as dilated cardiomyopathies, are not

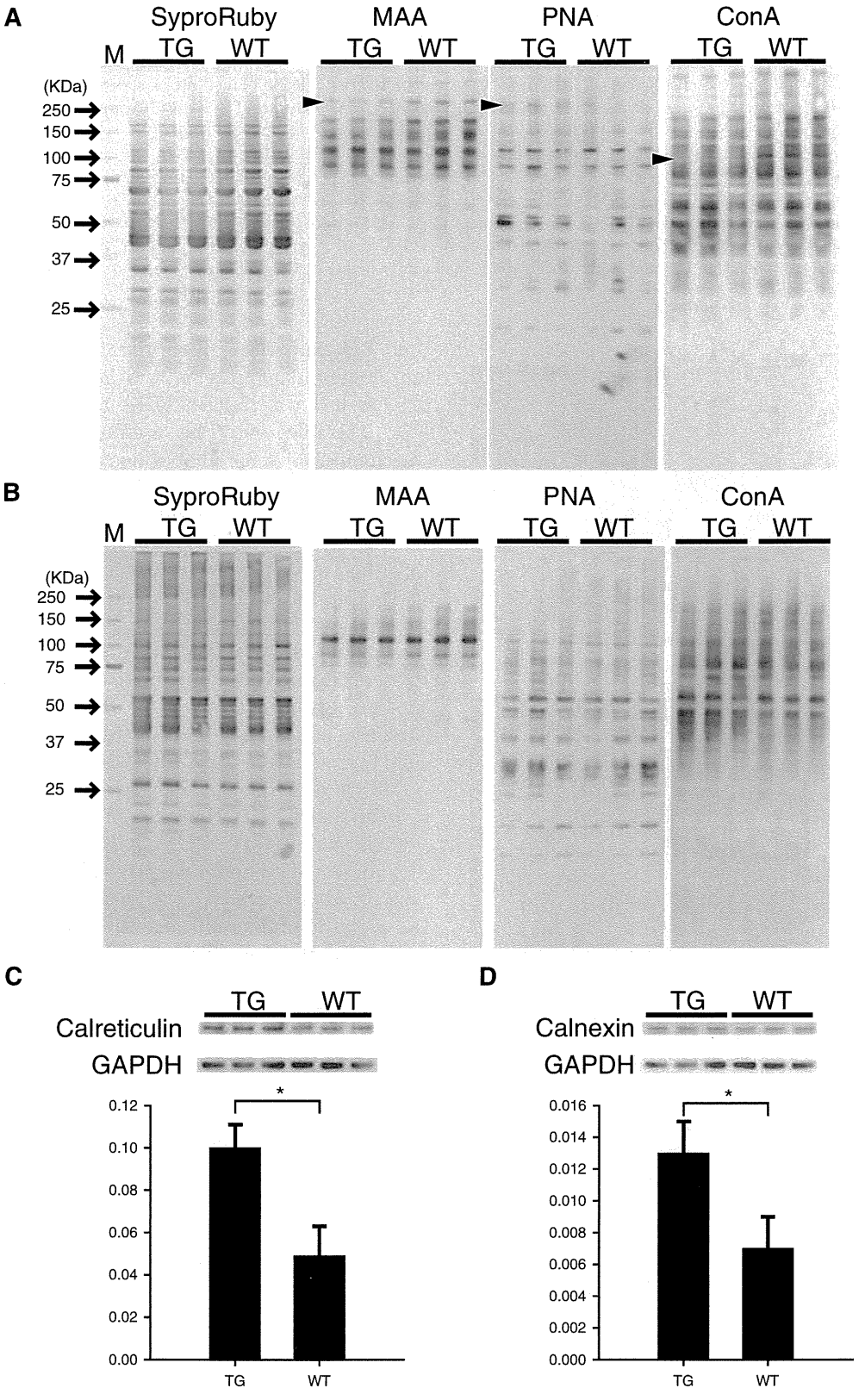

Fig. 6. *Continued on next page.*

Fig. 6. Lectin staining of two protein fractions extracted from the hearts of transgenic (TG) and wild-type (WT) mice ($n = 3$) at 10 weeks of age (A: fraction 1; B: fraction 2). After the confirmation of the presence of proteins on blot membranes by SyproRuby blot stain (one of three blots is shown for each fraction), the blots were stained with three lectins (ConA, MAA, PNA). Lectin binding was visualized with chemiluminescence. No evident difference was found on fraction 2 lectin blots containing proteins with lower solubility (*e.g.*, membrane proteins). However, some differentially stained bands (arrows) between TG and WT hearts were found in fraction 1 (soluble proteins): ~100 kDa by ConA, and ~250 kDa by MAA and PNA. ConA staining indicated that ~100 kDa proteins from TG hearts lost their high-mannose-type glycosylation, which was present in those of WT hearts. PNA staining, which recognizes Gal-GalNAc sugars, indicated that the sugar portion of the 250-kDa band in WT mice was highly sialylated, and less sialylated in TG mice. MAA staining, which recognizes α2,3-sialylation of sugars, such as Gal-GalNAc, confirmed higher sialylation of proteins of the same size in WT mice than TG mice. Thus, heart proteins in the TG mice were less sialylated than those of WT mice even though ST3Gal-II, one of the sialyltransferases, was overexpressed in the TG mice. M: Molecular weight markers. Western blots indicate that heart expression of calreticulin (C) and calnexin (D) were significantly higher in the TG hearts than that in WT hearts ($p < 0.05$).

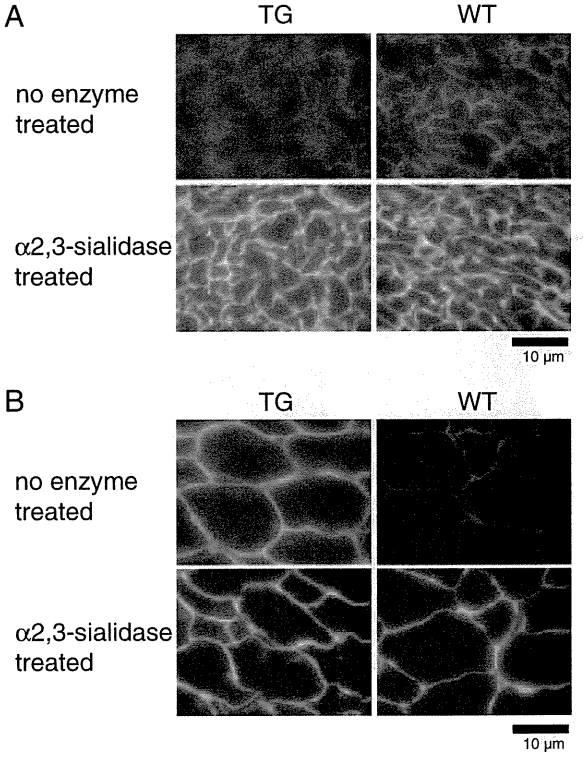

Fig. 7. Frozen sections of heart (A) and rectus femoris muscle (B) treated with or without α2,3-sialidase and stained with biotinylated PNA lectin, followed by FITC-avidin D. Bars = 10 μm. PNA binding was localized to pericellular regions without sialidase treatment, whereas the reactivity was essentially the same between TG and WG hearts. The reactivity in TG muscle was higher than in WT muscle. After sialidase treatment, PNA binding in both became evident equally in TG and WT heart and muscle.

fully understood. Some are known, such as inflammation of the myocardium in viral carditis and loss of or abnormalities in genes encoding structural proteins, particularly in hereditary cardiomyopathies.[19] However, other idiopathic cardiomyopathies occur, for which the causes remain unknown. Our TG mice had no apparent disruption of genes encoding cardiomuscular proteins and no inflammatory response in heart tissues. These features suggest that our TG mice may be useful for examining the mechanism of some idiopathic cardiomyopathies.

Ganglioside abnormalities are unlikely to cause heart symptoms in the TG mice because no apparent change in ganglioside composition was detected in TG hearts, contrary to our expectation that the overexpressed ST3Gal-II would increase the content of sialylated glycolipids, such as GD1a. The absence of ganglioside changes suggests that the substrate preference predicted by *in vitro* experiments[4] does not always coincide with the *in vivo* situation. The absence of changes may be because there is little GM1, a substrate for ST3Gal-II, in mouse hearts.[20] GM3 is a major ganglioside in both mouse and human hearts.[20),21] However, in human hearts, other gangliosides (GM1, GD1a, GD1b, and GT1b) are also detected by more sensitive assays with a GM1-specific choleragenoid.[21] Additionally, GM1 can act as a cardioprotectant against hypoxic damage in neonatal rat myocardial cells.[22] Thus, further analysis with more sensitive assays is needed to clarify the possible involvement of ganglioside abnormalities in cardiomyopathies.

In contrast to gangliosides, the glycosylation of heart glycoproteins was perturbed in TG mice, demonstrated by the protein and histochemical analyses with lectins. The effects of exogenous ST3Gal-II enzymes induced by transgenesis altered sugar portions of glycoproteins beyond the reaction catalyzed directly by the ST3Gal-II enzyme. However, sialylation changes in an abnormal state might be difficult to interpret because both skeletal and heart muscle tissues contain cytosolic sialidases with high activity at neutral pH.[23] Elevated ST3Gal-II activity induced by transgenesis in TG mice might cause tissue damage in hearts and skeletal muscles by higher sialylation. In contrast, if the cytosol is exuded

from damaged (necrotic/degenerated) tissue into interstitial spaces of the hearts and muscles, various cytosolic enzymes, including sialidases, may act on glycoproteins on the surface of adjacent muscle fibers, resulting in removal of terminal sialic acids from glycoproteins, particularly membrane-bound proteins. This tendency was evident in skeletal muscles (Fig. 7B). Complicated effects of exogenous ST3Gal-II are also suggested by transfection experiments of human ST3Gal-II in cell cultures.[24] In the experiments, the level of ST3Gal-II mRNA are not necessary consistent with those of monosialosyl globopentaosylceramide (MSGb5), a product catalyzed by ST3Gal-II.[24] Production of MSGb5 is highly dependent on cell types used for transfection, which may be due to cell-type-dependent sialidase activities.[24] In addition, altered protein glycosylation might be attributed to mislocalization of ST3Gal-II itself and/or the other glycosyltransferases in the Golgi apparatus by overloading of exogenous ST3Gal-II because expression-dependent mislocalizations were reported for glycosylation-related enzymes like α2,6-sialyltransferase,[25] GA2/GM2/GD2 synthase,[26] and human galactosyltransferase.[27] Thus, the perturbation in the glycoprotein sugar portions might have been caused by a complex imbalance of glycosylation–deglycosylation reactions in TG mice.

Elevated calreticulin and calnexin levels in TG hearts suggest that cardiac dilatation in TG mice is a response to ER-stress *via* elevated ERQC, caused by disorganized protein glycosylation in the ER/SR. Calreticulin and calnexin participate in a molecular chaperone system that integrates the processes of *N*-glycosylation and ERQC.[10] Calreticulin is a multifunctional protein involved in many functions, such as regulation of calcium homeostasis,[28] ERQC,[29] and interactions with various nuclear hormone receptors.[30] In the heart, calreticulin is highly expressed in the developing heart, but is strongly downregulated after birth.[31),32] The low level of calreticulin expression in adult heart is important for normal heart function because overexpression of calreticulin in the mouse heart leads to severe cardiac pathology, such as cardiac chamber dilatation,[33] resulting in complete heart block and sudden death.[34] These harmful effects of calreticulin overexpression may be due to various forms of ER stress.[35] Myocardiac cells overexpressing calreticulin are highly susceptible to apoptosis under oxidative stress.[36] The presence of underglycosylated proteins generates a signal leading to increased GRP78 gene expression,[37] which is an ER stress-associated protein.[38] Thus, ST3Gal-II overexpression in our TG mice might have perturbed protein glycosylation, which evoked ER stress and stimulated calreticulin expression, and the elevated calreticulin may have caused cardiac dilatation. However, the mechanism is not so simple, because calreticulin is not always elevated in dilated hearts; the calreticulin level is not influenced in some cases of human dilated cardiomyopathy.[39] Further investigations are needed to evaluate the involvement of calreticulin in TG hearts.

In conclusion, our transgenic mice (4C30 line) may represent a new form of cardiac dilatation with abnormal glycosylation. Although we do not yet have evidence for a direct connection between abnormal ST3Gal II expression and cardiac dilatation, our findings suggest that the glycosylation status of heart proteins should be evaluated carefully as a possible cause of DCM, especially noninflammatory cases, in humans. Our TG mice have potential as a new animal model for cardiac dilatation diseases, such as dilated cardiomyopathy, because the mice can be maintained as a homozygous line with 100% incidence of heart symptoms and a clear zygosity check system for the transgene allele is available.[14] The 4C30 strain is available from JCRB Laboratory Animal Resource Bank at the National Institute of Biomedical Innovation (http://animal.nibio.go.jp/).

Acknowledgments

We thank Dr. J. Miyazaki of Osaka University for the gift of the pCAGGS plasmid and K. Takano for technical assistance. This work was supported by a grant from the Ministry of Health, Labour and Welfare, Japan.

References

1) Richardson, P., McKenna, W., Bristow, M., Maisch, B., Mautner, B., O'Connell, J., Olsen, E., Thiene, G., Goodwin, J., Gyarfas, I., Martin, I. and Nordet, P. (1996) Report of the 1995 World Health Organization/International Society and Federation of Cardiology Task Force on the Definition and Classification of cardiomyopathies. Circulation **93**, 841–842.
2) Lee, Y.C., Kurosawa, N., Hamamoto, T., Nakaoka, T. and Tsuji, S. (1993) Molecular cloning and expression of Galβ1,3GalNAc α2,3-sialyltransferase from mouse brain. Eur. J. Biochem. **216**, 377–385.
3) Lee, Y.C., Kojima, N., Wada, E., Kurosawa, N., Nakaoka, T., Hamamoto, T. and Tsuji, S. (1994) Cloning and expression of cDNA for a new type of Galβ1,3GalNAc α2,3-sialyltransferase. J. Biol. Chem. **269**, 10028–10033.

4) Kono, M., Ohyama, Y., Lee, Y.C., Hamamoto, T., Kojima, N. and Tsuji, S. (1997) Mouse β-galactoside α2,3-sialyltransferases: comparison of *in vitro* substrate specificities and tissue specific expression. Glycobiology **7**, 469–479.
5) Fukumoto, S., Miyazaki, H., Goto, G., Urano, T. and Furukawa, K. (1999) Expression cloning of mouse cDNA of CMP-NeuAc:Lactosylceramide α2,3-sialyltransferase, an enzyme that initiates the synthesis of gangliosides. J. Biol. Chem. **274**, 9271–9276.
6) Okajima, T., Fukumoto, S., Miyazaki, H., Ishida, H., Kiso, M., Furukawa, K. and Urano, T. (1999) Molecular cloning of a novel α2,3-sialyltransferase (ST3Gal VI) that sialylates type II lactosamine structures on glycoproteins and glycolipids. J. Biol. Chem. **274**, 11479–11486.
7) Kojima, N., Lee, Y.C., Hamamoto, T., Kurosawa, N. and Tsuji, S. (1994) Kinetic properties and acceptor substrate preferences of two kinds of Galβ1,3-GalNAc α2,3-sialyltransferase from mouse brain. Biochemistry **33**, 5772–5776.
8) Ellies, L.G., Sperandio, M., Underhill, G.H., Yousif, J., Smith, M., Priatel, J.J., Kansas, G.S., Ley, K. and Marth, J.D. (2002) Sialyltransferase specificity in selectin ligand formation. Blood **100**, 3618–3625.
9) Kim, Y.J., Kim, K.S., Kim, S.H., Kim, C.H., Ko, J.H., Choe, I.S., Tsuji, S. and Lee, Y.C. (1996) Molecular cloning and expression of human Galβ1,3GalNAc α2,3-sialyltransferase (hST3Gal II). Biochem. Biophys. Res. Commun. **228**, 324–327.
10) Kopito, R.R. (1997) ER quality control: the cytoplasmic connection. Cell **88**, 427–430.
11) Michalak, M., Corbett, E.F., Mesaeli, N., Nakamura, K. and Opas, M. (1999) Calreticulin: one protein, one gene, many functions. Biochem. J. **344** (Pt 2), 281–292.
12) Wada, I., Rindress, D., Cameron, P.H., Ou, W.J., Doherty, J.J., Louvard, D., Bell, A.W., Dignard, D., Thomas, D.Y. and Bergeron, J.J. (1991) SSRα and associated calnexin are major calcium binding proteins of the endoplasmic reticulum membrane. J. Biol. Chem. **266**, 19599–19610.
13) Niwa, H., Yamamura, K. and Miyazaki, J. (1991) Efficient selection for high-expression transfectants with a novel eukaryotic vector. Gene **108**, 193–199.
14) Noguchi, A., Takekawa, N., Einarsdottir, T., Koura, M., Noguchi, Y., Takano, K., Yamamoto, Y., Matsuda, J. and Suzuki, O. (2004) Chromosomal mapping and zygosity check of transgenes based on flanking genome sequences determined by genomic walking. Exp. Anim. **53**, 103–111.
15) Folch, J., Lees, M. and Stanley, G.H.S. (1957) A simple method for the isolation and purification of total lipides from animal tissues. J. Biol. Chem. **226**, 497–509.
16) Williams, M.A. and McCluer, R.H. (1980) The use of Sep-Pak C18 cartridges during the isolation of gangliosides. J. Neurochem. **35**, 266–269.
17) Svennerholm, L. (1957) Quantitative estimation of sialic acids. II. A colorimetric resorcinol-hydrochloric acid method. Biochim. Biophys. Acta **24**, 604–611.
18) Sakamoto, A., Ono, K., Abe, M., Jasmin, G., Eki, T., Murakami, Y., Masaki, T., Toyo-oka, T. and Hanaoka, F. (1997) Both hypertrophic and dilated cardiomyopathies are caused by mutation of the same gene, δ-sarcoglycan, in hamster: an animal model of disrupted dystrophin-associated glycoprotein complex. Proc. Natl. Acad. Sci. U. S. A. **94**, 13873–13878.
19) Towbin, J.A. and Bowles, N.E. (2002) The failing heart. Nature **415**, 227–233.
20) Leskawa, K.C. and Short, C.S. (1988) Glycolipids of cardiac muscle: an interspecies comparison. Glycoconj. J. **5**, 302.
21) Müthing, J. and Čačić, M. (1997) Glycosphingolipid expression in human skeletal and heart muscle assessed by immunostaining thin-layer chromatography. Glycoconj. J. **14**, 19–28.
22) Jin, Z.Q., Zhou, H.Z., Zhu, P., Honbo, N., Mochly-Rosen, D., Messing, R.O., Goetzl, E.J., Karliner, J.S. and Gray, M.O. (2002) Cardioprotection mediated by sphingosine-1-phosphate and ganglioside GM-1 in wild-type and PKCε knockout mouse hearts. Am. J. Physiol. Heart Circ. Physiol. **282**, H1970–H1977.
23) Dairaku, K., Miyagi, T., Wakui, A. and Tsuiki, S. (1986) Cytosolic sialidases of rat tissues with special reference to skeletal muscle enzyme. Biochem. Int. **13**, 741–748.
24) Saito, S., Aoki, H., Ito, A., Ueno, S., Wada, T., Mitsuzuka, K., Satoh, M., Arai, Y. and Miyagi, T. (2003) Human α2,3-sialyltransferase (ST3Gal II) is a stage-specific embryonic antigen-4 synthase. J. Biol. Chem. **278**, 26474–26479.
25) Rabouille, C., Hui, N., Hunte, F., Kieckbusch, R., Berger, E.G., Warren, G. and Nilsson, T. (1995) Mapping the distribution of Golgi enzymes involved in the construction of complex oligosaccharides. J. Cell Sci. **108**, 1617–1627.
26) Giraudo, C.G., Rosales Fritz, V.M. and Maccioni, H.J. (1999) GA2/GM2/GD2 synthase localizes to the trans-Golgi network of CHO-K1 cells. Biochem. J. **342**, 633–640.
27) Teasdale, R.D., Matheson, F. and Gleeson, P.A. (1994) Post-translational modifications distinguish cell surface from Golgi-retained β1,4 galactosyltransferase molecules. Golgi localization involves active retention. Glycobiology **4**, 917–928.
28) Michalak, M., Robert Parker, J.M. and Opas, M. (2002) Ca^{2+} signaling and calcium binding chaperones of the endoplasmic reticulum. Cell Calcium **32**, 269–278.
29) Zapun, A., Darby, N.J., Tessier, D.C., Michalak, M., Bergeron, J.J. and Thomas, D.Y. (1998) Enhanced catalysis of ribonuclease B folding by the interaction of calnexin or calreticulin with ERp57. J. Biol. Chem. **273**, 6009–6012.
30) Dedhar, S., Rennie, P.S., Shago, M., Hagesteijn, C.Y., Yang, H., Filmus, J., Hawley, R.G., Bruchovsky, N., Cheng, H., Matusik, R.J. and

Giguère, V. (1994) Inhibition of nuclear hormone receptor activity by calreticulin. Nature **367**, 480–483.

31) Mesaeli, N., Nakamura, K., Zvaritch, E., Dickie, P., Dziak, E., Krause, K.H., Opas, M., MacLennan, D.H. and Michalak, M. (1999) Calreticulin is essential for cardiac development. J. Cell Biol. **144**, 857–868.

32) Papp, S., Zhang, X., Szabo, E., Michalak, M. and Opas, M. (2008) Expression of endoplasmic reticulum chaperones in cardiac development. Open Cardiovasc. Med. J. **2**, 31–35.

33) Hattori, K., Nakamura, K., Hisatomi, Y., Matsumoto, S., Suzuki, M., Harvey, R.P., Kurihara, H., Hattori, S., Yamamoto, T., Michalak, M. and Endo, F. (2007) Arrhythmia induced by spatiotemporal overexpression of calreticulin in the heart. Mol. Genet. Metab. **91**, 285–293.

34) Nakamura, K., Robertson, M., Liu, G., Dickie, P., Guo, J.Q., Duff, H.J., Opas, M., Kavanagh, K. and Michalak, M. (2001) Complete heart block and sudden death in mice overexpressing calreticulin. J. Clin. Invest. **107**, 1245–1253.

35) Kageyama, K., Ihara, Y., Goto, S., Urata, Y., Toda, G., Yano, K. and Kondo, T. (2002) Overexpression of calreticulin modulates protein kinase B/Akt signaling to promote apoptosis during cardiac differentiation of cardiomyoblast H9c2 cells. J. Biol. Chem. **277**, 19255–19264.

36) Ihara, Y., Urata, Y., Goto, S. and Kondo, T. (2006) Role of calreticulin in the sensitivity of myocardiac H9c2 cells to oxidative stress caused by hydrogen peroxide. Am. J. Physiol. Cell Physiol. **290**, C208–C221.

37) Chang, S.C., Wooden, S.K., Nakaki, T., Kim, Y.K., Lin, A.Y., Kung, L., Attenello, J.W. and Lee, A.S. (1987) Rat gene encoding the 78-kDa glucose-regulated protein GRP78: its regulatory sequences and the effect of protein glycosylation on its expression. Proc. Natl. Acad. Sci. U. S. A. **84**, 680–684.

38) Shintani-Ishida, K., Nakajima, M., Uemura, K. and Yoshida, K. (2006) Ischemic preconditioning protects cardiomyocytes against ischemic injury by inducing GRP78. Biochem. Biophys. Res. Commun. **345**, 1600–1605.

39) Meyer, M., Schillinger, W., Pieske, B., Holubarsch, C., Heilmann, C., Posival, H., Kuwajima, G., Mikoshiba, K., Just, H. and Hasenfuss, G. (1995) Alterations of sarcoplasmic reticulum proteins in failing human dilated cardiomyopathy. Circulation **92**, 778–784.

(Received Apr. 1, 2011; accepted June 13, 2011)

Journal of Neurochemistry

JOURNAL OF NEUROCHEMISTRY | 2011 | 118 | 399–406

doi: 10.1111/j.1471-4159.2011.07310.x

ORIGINAL ARTICLE

Lysosomal accumulation of Trk protein in brain of G_{M1}-gangliosidosis mouse and its restoration by chemical chaperone

Ayumi Takamura,*[,1] Katsumi Higaki,* Haruaki Ninomiya,† Tomoko Takai,* Junichiro Matsuda,‡ Masami Iida,§ Kousaku Ohno,¶ Yoshiyuki Suzuki** and Eiji Nanba*

*Division of Functional Genomics, Research Center for Bioscience and Technology, Nishi-cho, Yonago, Japan

†Department of Biological Regulation, School of Health Science, Faculty of Medicine, Nishi-cho, Yonago, Japan

‡National Institute of Biomedical Innovation, Saito-asagi, Ibaraki, Japan

§Central Research Laboratories, Seikagaku Corporation, Tateno, Higashi-Yamano, Tokyo, Japan

¶Division of Child Neurology, Department of Neurological Science, Tottori University Faculty of Medicine, Nishi-cho, Yonago, Japan

**International University of Health and Welfare Graduate School, Kita-Kanemaru, Otawara, Japan

Abstract

G_{M1}-gangliosidosis is a fatal neurodegenerative disorder caused by deficiency of lysosomal acid β-galactosidase (β-gal). Accumulation of its substrate ganglioside G_{M1} (G_{M1}) in lysosomes and other parts of the cell leads to progressive neurodegeneration, but underlying mechanisms remain unclear. Previous studies demonstrated an essential role for interaction of G_{M1} with tropomyosin receptor kinase (Trk) receptors in neuronal growth, survival and differentiation. In this study we demonstrate accumulation of G_{M1} in the cell-surface rafts and lysosomes of the β-gal knockout (β-gal−/−) mouse brain association with accumulation of Trk receptors and enhancement of its downstream signaling. Immunofluorescence and subcellular fractionation analysis revealed accumulation of Trk receptors in the late endosomes/lysosomes of the β-gal−/− mouse brain and their association with ubiquitin and p62. Administration of a chemical chaperone to β-gal−/− mouse expressing human mutant R201C protein resulted in a marked reduction of intracellular storage of G_{M1} and phosphorylated Trk. These findings indicate that G_{M1} accumulation in rafts causes activation of Trk signaling, which may participate in the pathogenesis of G_{M1}-gangliosidosis.

Keywords: chemical chaperone, G_{M1}-gangliosidosis, lysosome, neurodegeneration, Trk receptor.

J. Neurochem. (2011) **118**, 399–406.

G_{M1}-gangliosidosis is a neurodegenerative glycosphingolipid storage disorder caused by genetic deficiency of lysosomal β-galactosidase (β-gal) with consequent disruption of the degradative pathway of ganglioside G_{M1} (G_{M1}) (Suzuki *et al.* 2008). Clinically, infantile, juvenile and adult/chronic forms are distinguished by the age of onset. The residual β-gal activity in affected individual correlates with the onset and rate of progression of the disease. Storage of G_{M1} leads to the onset of pathology of this disease, but the pathophysiological mechanism of neurodegeneration remain elusive (Brunetti-Pierri and Scaglia 2008). Once undegraded substrate starts to accumulate, it builds up within lysosomes until it becomes the maximum level, and then the storage extends to other parts of the cells, such as the endoplasmic reticulum

Received February 25, 2011; revised manuscript received May 9, 2011; accepted May 10, 2011.

Address correspondence and reprint requests to Katsumi Higaki, Associate Professor, Division of Functional Genomics, Research Center for Bioscience and Technology, Tottori University, 86 Nishi-cho, Yonago, 683-8503, Japan. E-mail: kh4060@med.tottori-u.ac.jp

[1]The present address of Ayumi Takamura is the Department of Neurology, Institute of Brain Science, Hirosaki University Graduate School of Medicine, Hirosaki, Japan.

Abbreviations used: β-gal, β-galactosidase; BSA, bovine serum albumin; DRMs, detergent-resistant membrane microdomains; ER, endoplasmic reticulum; G_{M1}, ganglioside G_{M1}; GSLs, glycosphingolipids; IP, immunoprecipitation; NGF, nerve growth factor; NOEV, *N*-octyl-4-epi-β-valienamine; PBS, phosphate buffered saline; pErk, phosphorylated Erk; PLCγ, phospholipase C γ; PM, plasma membrane; pTrk, phosphorylated Trk; Trk, tropomyosin receptor kinase; Ub, ubiquitin; WT, wild type.

(ER), Golgi apparatus and plasma membrane (PM) (Walkley and Vanier 2009).

Gangliosides are components of the cell membranes, and are particularly abundant in the neuronal surface of the brain (Posse de Chaves and Sipione 2010). Striking changes in synthesis and expression of gangliosides have been observed during brain development, which is though to play critical roles in cell differentiation, proliferation and death (Yu *et al.* 2004). G_{M1} is one of the major gangliosides in the vertebrate brain and it acts as a pleiotropic neurotrophic factor to promote neuronal growth, differentiation and survival after brain injury (Schönhöfer 1992; Ferrari *et al.* 1995). It is also known to enhance the activity of nerve growth factor (NGF) on NGF-responsive cells and stimulated neurite outgrowth *in vivo* and *in vitro* by enhancing NGF-induced autophosphorylation of the high affinity NGF receptor, tropomyosin receptor kinase (Trk) receptor (Duchemin *et al.* 2002). This enhancing effect of G_{M1} is thought at least partly attributable to its physical and functional association with Trk protein (Mutoh *et al.* 1995). It also enhances NGF-induced Trk receptor-dimerization, and its tyrosine phosphorylation. Phosphorylated Trk (pTrk) binds to downstream signaling molecules such as phospholipase C γ (PLCγ), Shc and phosphatidyl inositol 3-kinase (Duchemin *et al.* 2008).

Binding of NGF to its receptor TrkA induces ubiquitination and subsequent internalization of TrkA to endocytic vesicles (Geetha *et al.* 2005; Wooten *et al.* 2008). Once internalized into early endosomes, TrkA may either recycle to the plasma membrane through recycling endosomes or it may enter the degradative pathway through multivesicular bodies to be degraded in lysosomes. In our previous study, we demonstrated impairment of autophagy in neurons and astrocytes from G_{M1}-gangliosidosis model mice (Takamura *et al.* 2008). It was suggested that storage of undegraded cytoplasmic organelle and ubiquitinated proteins disrupt neuronal function and ultimately lead to neurodegeneration.

In the present study, we examined an involvement of neurotrophin signaling in the brain pathology of G_{M1}-gangliosidosis mice. We found enhanced phosphorylation of Trk protein in the β-gal knockout mouse brain. When a chemical chaperone therapy was evaluated in mice expressing mutant human β-gal (R201C), the treated animals showed marked reduction in the level of pTrk. These results indicate alternation of Trk receptor signaling in G_{M1}-gangliosidosis mouse brain, which may contribute to the pathogenesis of this disease.

Materials and methods

Materials

Mouse monoclonal antibodies against G_{M1} (GMB16), asialo G_{M1} (G_{A1}) (AG-1) and G_{M2} were obtained from Seikagaku Corporation (Tokyo, Japan). Rabbit polyclonal anti-TrkA (H-190 and 763), anti-TrkB (794), anti-caveolin-1 (H-97), anti-β-tubulin (H-235), mouse monoclonal anti-pTrk (E-6) and anti-Ubiquitin (Ub) (P4D1) were from Santa Cruz Biotechnology Inc. (Santa Cruz, CA, USA). Mouse monoclonal anti-PLCγ (05-163) and anti-phosphotyrosine (4G10) were from Upstate Biotechnology (Lake Placid, NY, USA). Rabbit polyclonal anti-Erk and phosphorylated Erk (pErk) were from Cell Signaling (Beverly, MA, USA). Rabbit polyclonal anti-p62/SQSTM1 (PM045) was from MBL Co. Ltd (Nagoya, Japan). Alexa Fluor 488 and Alexa Fluor 555-conjugated secondary antibodies were from Molecular Probes, Inc. (Invitrogen Corp., Carlsbad, CA, USA). Rabbit polyclonal anti-calnexin, anti-lysosomal-associated membrane protein 2 (LAMP2) and filipin complex was from Sigma-Aldrich (St Louis, MO, USA).

Mice and tissue collection

C57BL/6-based congenic strain with β-gal knockout (β-gal−/−) mice and those expressing human mutant R201C enzyme (R201C mice) have been reported previous (Matsuda *et al.* 1997, 2003). All procedures were carried out according to the protocols approved by the committee for animal experiments in Tottori University. For immunostaining, mice were anesthetized and perfused with 4% paraformaldehyde in sodium phosphate, pH 7.4. Brains were embedded in OCT compound (Sakura Finetechnical Co., Tokyo, Japan), and 8-μm sections were cut using a cryostat. For protein extractions, tissues were removed and frozen in liquid nitrogen. R201C mice were treated with *N*-octyl-4-epi-β-valienaline (NOEV) in an aqueous solution (0.1 mM) orally for 16 weeks (Suzuki *et al.* 2007). Untreated mice were given water.

Primary neuronal cell culture from neonatal mouse brain

Primary cerebellar granule neurons were prepared as reported previously (Kiedrowski *et al.* 2004). Briefly, cerebella were isolated from postnatal 7 days mice, and washing with ice-cold cultured medium (Dulbecco's modified Eagle's medium/F12 with 10% fetal bovine serum (FBS), 25 mM KCl and 10 mg/mL gentamicin). Granule cells were dissociated by 10-min incubation with 0.1% trypsin solution, DNase I and triturated with Pasteur pipettes. The cells plated in poly-L-lysine-coated plastic dishes at the density of 2×10^5 cells per 35-mm dish with cultured medium. Then the cells were cultured for 7 days with 20 mM cytosine arabinoside.

Immunofluorescence

All the procedures were carried out at 20°C as described previously (4). Cultured neuronal cells were fixed with 4% paraformaldehyde in phosphate buffered saline (PBS) for 30 min. Cells or brain sections were permeabilized with 0.25% Triton X-100 in PBS for 15 min, blocked with 1% bovine serum albumin (BSA) for 1 h, and incubated with primary antibodies for 1 h. We used anti-G_{M1} and G_{A1} at 1 : 50 dilution with 0.1% BSA/PBS, anti-TrkA, TrkB, pTrk and caveolin-1 at 1 : 100 dilution and anti-Ub at 1 : 250 dilution, respectively. Bound antibodies were detected with Alexa-Fluor-conjugated secondary antibodies (1 : 2000 in 0.1% BSA/PBS) for 1 h. For staining of G_{M1} in the plasma membrane of cultured cells, cells were incubated with anti-G_{M1} without Triton X-100 treatment. For detection of free cholesterol, cells or brain sections were washed with PBS and incubated with 300 μg/mL of filipin in PBS for 1 h. Samples were mounted on slideglass with Vectashield mounting media (Vector Laboratories, Burlingame, CA, USA) and fluorescence images were obtained sequentially using a confocal laser microscopy

(Leica TSC SP-2, Wetzler, Germany). Fluorescence intensity was measured using Leica confocal software.

Immunoprecipitation and immunoblotting

All the procedures were carried out at 4°C. The cerebral cortex was lysed by sonication in 10 mM Tris–HCl (pH 7.4), 150 mM NaCl, 1 mM EDTA, 1 mM EGTA, and a protease inhibitor cocktail (Roche Molecular Biochemicals, Indianapolis, IN, USA). Triton X-100 (1%) insoluble extracts or detergent-resistant membrane microdomains (DRMs) were obtained as below. Briefly, lysates from the cortex were incubated with Triton X-100 (1% v/v) and incubated on ice for 30 min, and insoluble fractions were removed by centrifugation at 100 000 *g* for 30 min. The pellets were suspended in the same extraction buffer. Protein concentrations were determined using the Protein Assay Rapid kit (WAKO, Tokyo, Japan). Immunoprecipitation was carried out by using Catch and Release v2.0 (Upstate). Western blotting was performed as described (Takamura *et al.* 2008). Signals from horseradish peroxidase-conjugated secondary antibodies were visualized by ECL detection kit (GE Healthcare Bioscience, Little Chalfond, UK). For detection of G_{M1}, lysates were transferred onto nitrocellulose membrane using a dot blotter (Bio-Rad Laboratories, Hercules, CA, USA), and the membranes were probed with anti-G_{M1}. Blot densities were analyzed using the Image J software (National Institute of Health, Bethesda, MD, USA).

Cell fractionation and lipid analysis

Brain samples were lysed by sonication in 10 mM Tris–HCl (pH 7.4), 150 mM NaCl, 1 mM EDTA, 1 mM EGTA, 1% Triton X-100 and a protease inhibitor cocktail (Roche Diagnostics) and the supernatants were used as total extracts. For subcellular fractionation, extracted proteins were subjected to continuous gradient ultracentrifugation (90 000 *g* for 20 h at 4°C in SW 41Ti rotor) in Opti-prep gradient (Axis-Shield, Oslo, Norway) as described (Sugii *et al.* 2003). The top 22 fractions of the gradients were recovered and subjected to lipid analyses. For detection of G_{M1}, the fractions were transferred to a nitrocellulose membrane (Bio-Rad) using Bio-Dot microfiltration unit (Bio-Rad) and the membrane was probed with anti-G_{M1} for 1 h. Cholesterol concentration was determined with Amplex red cholesterol assay kit (Molecular probes) and phospholipids concentration was determined with phospholipids determination kit (WAKO).

Results

Storage of G_{M1} in lipid rafts of β-gal−/− mouse brain

β-Gal−/− mice are apparently healthy within 4 months after birth. Thereafter, they develop a progressive neurological disease characterized by tremor, ataxia, and abnormal gait, with an eventual demise at 7–10 months (Matsuda *et al.* 1997). Brain histochemistry revealed Periodic acid-Schiff (PAS)-positive intracytoplasmic storage and multilamellar inclusion bodies in neuronal cells at 5 months old, similar to those reported in human G_{M1}-gangliosidosis. Immunofluorescence with anti-G_{M1} revealed massive lysosomal accumulation of G_{M1} in cortical neurons of affected mice at 5 months old (Fig. 1a). Dot blot analysis of whole lysates (data not shown) and DRMs from the cerebral cortex revealed a marked increase of G_{M1} in the affected mice (3.8 + 0.4-fold increase in DRMs; $p < 0.01$) compared to the wild type (WT) (Fig. 1b and c). G_{A1} was also increased in the affected mice (data not shown). We also examined the concentrations of cholesterol and phospholipids in the DRMs of the brain. The concentration of cholesterol in the β-gal−/− mouse brain was significantly higher than that in the WT mouse brain, whereas that of phospholipids was indistinguishable between the two groups (Fig. 1d). When the plasma membrane of primary-cultured cerebellar granule cells were stained with anti-G_{M1} and anti-calnexin, G_{M1} was observed throughout plasma membrane of β-gal−/− cells. The signals were obviously higher than in WT cells (Fig. 2a) and co-localized with these of caveolin-1 (Fig. 2b), a marker protein for lipid raft (Manninen *et al.* 2005).

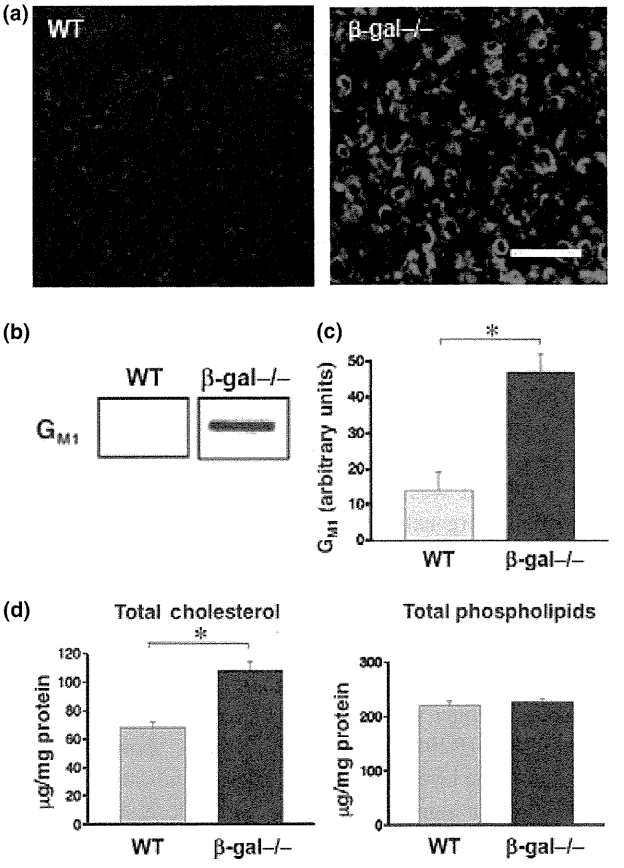

Fig. 1 Accumulation of G_{M1} and cholesterol in β-gal−/− mouse brain. (a) Anti-G_{M1} immunofluorescence of cortical sections from WT and β-gal−/− mouse (8 months old). Scale bar, 50 μm. (b, c) Triton X-100 insoluble fractions from WT and β-gal−/− mice were examined with anti-G_{M1}. (d) Levels of cholesterol and phospholipids in mouse brain. Whole brain lysates form WT and β-gal−/− mice were analyzed and the concentrations of total cholesterol and phospholipids were determined as described in Materials and methods. Each bar represents means ± SEM of three determinations, $n = 3$, $^*p < 0.01$.

Trk receptor signaling in the β-gal−/− mouse brain

Ganglioside G_{M1} interacts with Trk receptors to potentiate its neurotrophic effect (Mutoh *et al.* 1995). Specifically, it enhances NGF-induced tyrosine phosphorylation and activation of TrkA *in vitro* and *in vivo*. Therefore, we examined TrkA signaling in the β-gal−/− mouse brain. DRMs of the brains from 8-month-old WT and β-gal−/− mice were subjected to immunoprecipitation (IP) with anti-TrkA or anti-pTrk antibodies, followed by immunoblotting with anti-G_{M1}. The IP experiments revealed increased levels of G_{M1} bound to TrkA and pTrk in the β-gal−/− mouse brain (Fig. 3a and b). No association of G_{M2} with TrkA and pTrk was found either in the WT and the β-gal−/− mouse brains. Increased levels of Trk and pTrk proteins was also observed in the DRMs fraction of the β-gal−/− mice brain (Fig. 4a). Immunofluorescence with anti-TrkA and anti-pTrk revealed high levels of these proteins in the β-gal−/− mouse cortex, in contrast to the virtual absence of the immunoreactivity in the WT brain (Fig. 4b). TrkA in the β-gal−/− mouse cortex was predominantly localized to the cytoplasm, where it co-localized with G_{M1} (Fig. 4c). pTrk binds to effector molecules Shc, PLCγ and phosphatidyl inositol 3-kinase causing their phosphorylation and activation of intracellular signaling pathways (Duchemin *et al.* 2008). IP experiments revealed increased levels of pTrk bound to PLCγ in the β-gal−/− mouse brain (Fig. 4d). The level of pErk was also increased in the β-gal−/− mouse brain (Fig. 4e).

Lysosomal accumulation of ubiquitinated Trk protein in the β-gal−/− mouse brain

The level of Trk protein is regulated by internalization and retrograde transport to the endosomes/lysosomes, where it is degraded (Wooten *et al.* 2008). Because this sorting is regulated by ubiquitination, we examined the levels of ubiquitinated Trk in the β-gal−/− mouse brain. Immunofluorescence showed that ubiquitin signals co-localized with those of TrkA and lysosomal-associated membrane protein 2 (LAMP2) immunoreactivity in the cerebral cortex of the β-gal−/− mouse (Fig. 5a and b). Anti-Ub IP products from the β-gal−/− brain extracts contained TrkA and TrkB, suggesting ubiquitination of those proteins (Fig. 5c). Anti-p62 IP products also contained TrkA and TrkB.

To separate the endosomal/lysosomal compartments from the PM, we performed subcellular fractionation of whole brain lysates using Optiprep gradient. Immunoblot analyses of WT fractions demonstrated localization of G_{M1} mainly in the PM (N^+K^+-ATPase positive fractions #4–8), and that of TrkA, TrkB and pTrk in both the PM and the late endosomes/lysosomes (Fig. 6a and c). In contrast, G_{M1} was broadly distributed in the heavier fractions (Rab7 positive fractions #11–21) from β-gal−/− mouse brain and TrkA, TrkB and pTrk were predominantly redistributed to endosomal/lysosomal fractions. Anti-Ub immunoblotting showed clear signals of ubiquitin in the endosomal/lysosomal fractions of the β-gal−/− brain, but not in that of the WT brain (Fig. 6b).

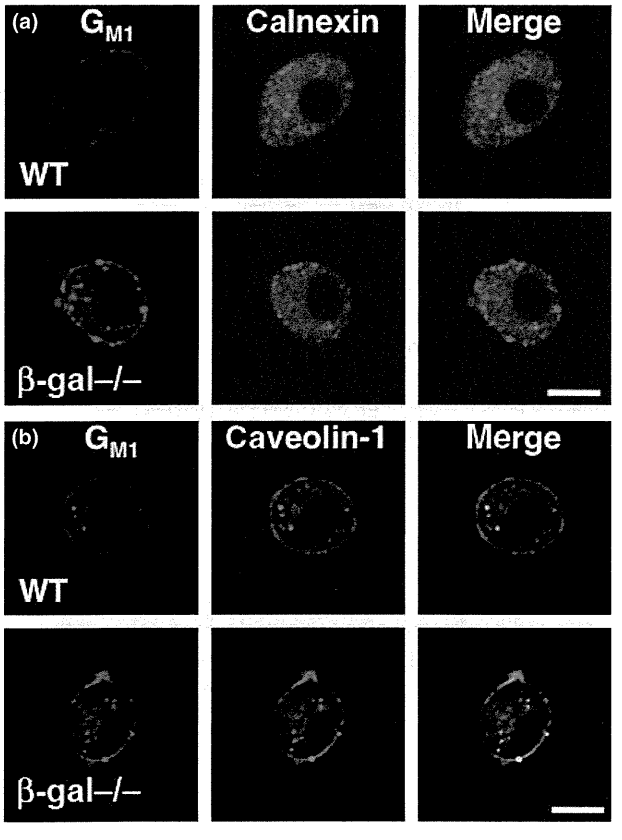

Fig. 2 Accumulation of G_{M1} in the PM of β-gal−/− granule cells. Cerebellar granule cells were prepared from brain from WT and β-gal−/− mice and subjected to immunostaining with anti-G_{M1}, anti-calnexin and anti-caveolin-1 as described in Materials and methods. Images were obtained by signal stacks. (a) Distribution of G_{M1} in the PM of cultured granule cells. (b) Co-localization of G_{M1} with caveolin-1in the PM of cultured granule cells. Scale bars, 20 μm.

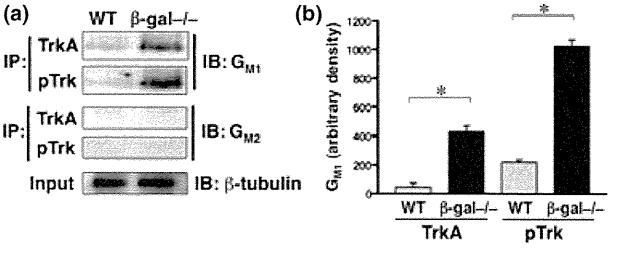

Fig. 3 Increased association of G_{M1} and Trk proteins in lysates from β-gal−/− mouse brain. Triton X-100 insoluble extractions of WT and β-gal−/− mice were subjected to the assays. (a) Detections of G_{M1} and G_{M2} in TrkA and pTrk immunoprecipitates. Total extract input was detected by β-tubulin. (b) Densities of G_{M1} in TrkA and pTrk immunoprecipitates were quantified. Values are mean ± SEM, $n = 3$, $^*p < 0.01$.

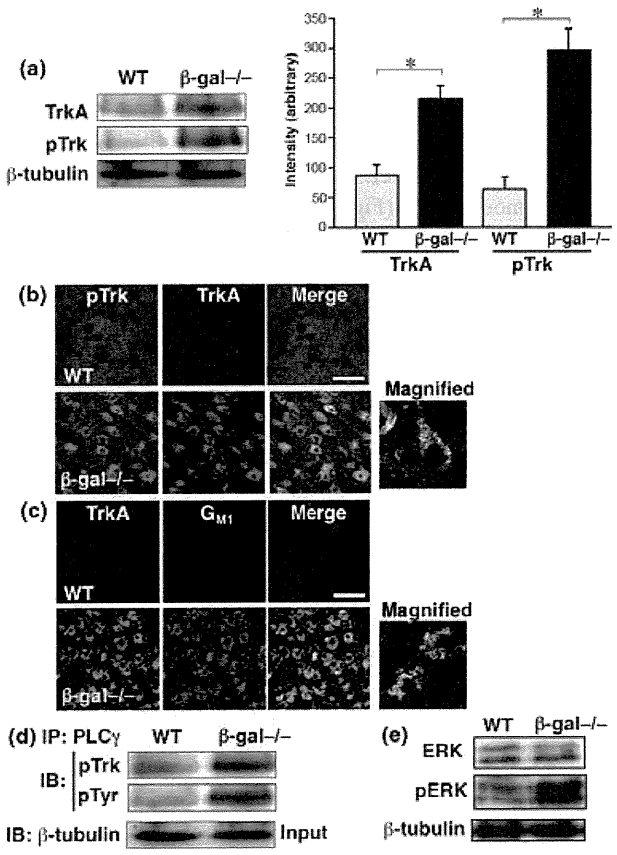

Fig. 4 Enhanced Trk receptor signaling in β-gal–/– mouse brain. Triton X-100 insoluble extractions of WT and β-gal–/– mice were subjected to immunoblotting and immunoprecipitation. (a) Immunoblotting with anti-TrkA, pTrk and β-tubulin (as loading controls) and quantification of immunoreactivities. Values are mean ± SEM, $n = 3$, $^*p < 0.01$. (b, c) Immunostaining of cortical sections from WT and β-gal–/– mice with indicated antibodies. Scale bars, 50 μm. (d) Immunoprecipitants with anti-PLCγ were immunoblotted with anti-pTrk and phospho-tyrosine (pTyr). Total extract input was detected by β-tubulin. (e) Immunoblotting with anti-ERK, pERK and β-tubulin.

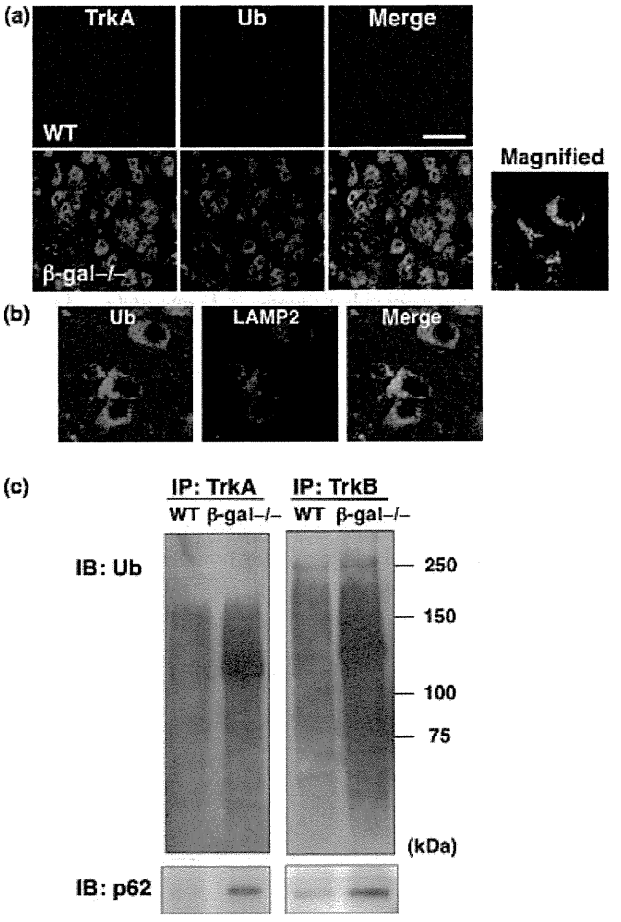

Fig. 5 Ubiquitination of Trk proteins in β-gal–/– mouse brain. (a) Sections from cerebral cortex of WT and β-gal–/– mice were stained with anti-TrkA and Ub. Scale bar, 50 μm. (b) Sections from cerebral cortex of β-gal–/– mice was stained with anti-Ub and lysosomal-associated membrane protein 2 (LAMP2). (c) Whole brain extracts from WT and β-gal–/– mice were immunoprecipitated with anti-TrkA and TrkB and then immunoblotted with anti-Ub and p62.

Effect of a chemical chaperone on Trk accumulation in the R201C mouse brain

We have previously reported that oral administration of a chaperone compound, NOEV, to the R201C mice increased β-gal activity and reduced G_{M1} accumulation in their brains (Matsuda *et al.* 2003; Suzuki *et al.* 2007). To determine whether NOEV decreases pTrk accumulation, sections from NOEV-treated R201C mice and untreated controls (10 months of age) were immunostained with antibodies against G_{M1}, G_{A1} and pTrk. NOEV caused a clear decrease of G_{M1}, G_{A1} and pTrk in neurons of the R201C mice (Fig. 7a and b). Filipin staining revealed cholesterol storage in neurons of the R201C mouse brain, which was also reduced by NOEV treatment. NOEV also reduced the levels of pTrk, pERK and cholesterol content in lysates from R201C mouse brain (Fig. 7c and d).

Discussion

Ganglioside G_{M1} is particularly abundant in the nervous system and has been shown to promote neuronal growth and differentiation in cell cultures and to protect injured and aged neurons in animal models (Schönhöfer 1992; Ferrari *et al.* 1995). These actions of G_{M1} are at least partly attributable to its physical and functional association with Trk neurotrophin receptors (Mutoh *et al.* 1995). G_{M1} also activates Trk receptors by inducing neurotrophin release (Rabin *et al.* 2002). G_{M1} has a trophic action on a broad repertoire of neurons in the CNS, which may imply a possible interaction with other Trk receptors, TrkB and TrkC (Duchemin *et al.* 2002). Over-expression of G_{M1}, however, suppressed NGF signals in PC12 cells, suggesting a requirement for a proper control of G_{M1} concentration (Nishio *et al.* 2004).

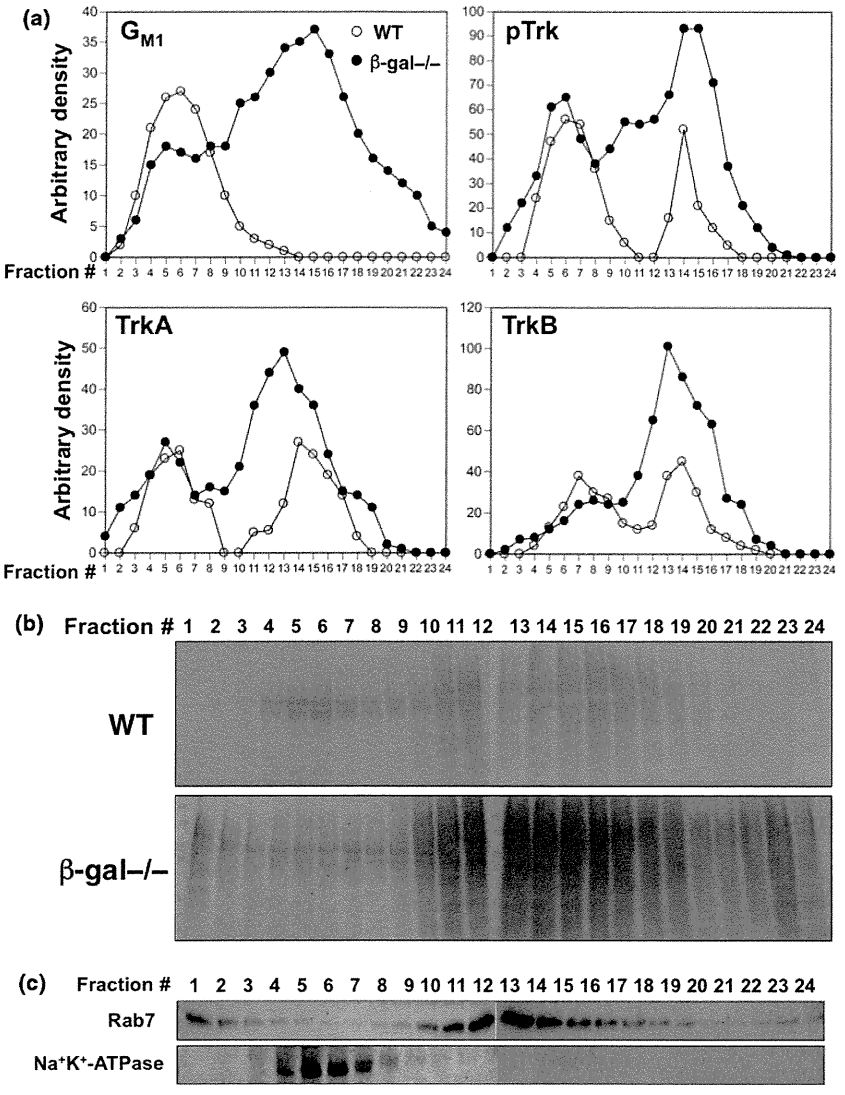

Fig. 6 Subcellular distribution of Trk proteins in β-gal–/– mouse brain. Whole brain lysates from WT and β-gal–/– mice 8M littermates were fractionated on an Opti-prep gradient as described in Materials and methods. Fractions were subjected to immunoblot analysis with anti-Rab7 (a marker for the late endosomes and lysosomes), Na^+-K^+-ATPase (for the PM), TrkA, pTrk, and Ub, respectively. They were also subjected to dot blot analysis with anti-G_{M1}. (a) The distributions of G_{M1}, pTrk, TrkA and TrkB are presented as the densities of blots. (b) Immunoblotting of fractions with anti-Ub. Results were representative of two independent experiments. (c) Immunoblotting of fractions from wt with anti-Rab7 and Na^+-K^+-ATPase. The same results were obtained using β-gal-deficient mice.

In this study, we investigated neurotrophin signals in the β-gal–/– mouse brain and found of Trk/G_{M1} association, Trk phosphorylation and downstream signaling events. Trk accumulated in the late endosomes/lysosomes in neurons of the affected mouse brains, and was highly ubiquitinated. When effects of NOEV on R201C mice were examined, in addition to a reduction of lipid storage, NOEV reduced pTrk accumulation. These findings suggest abnormal activation of Trk signaling in the G_{M1}-gangliosidosis mouse brain.

Studies on the endocytic itinerary of glycosphingolipids (GSLs) suggest that GSLs including G_{M1} are internalized from the PM via caveolae and are subsequently transported to the Golgi apparatus, whereas these lipids accumulate in endosomes/lysosomes of sphingolipid storage disease fibroblasts (Puri *et al.* 1999; Choudhury *et al.* 2006). Neurotrophins induce internalization of Trk receptor to the endosomes, where they are catalytically active and phosphorylated, and are less vulnerable to membrane associated phosphatases (Geetha *et al.* 2005; Wooten *et al.* 2008). Neurotrophin binding to Trk receptors stimulates activation of signaling intermediates such as PLCγ and Shc (Duchemin *et al.* 2008). Trk signaling and internalization was enhanced in G_{M1}-gangliosidosis mouse brains, perhaps because of the accumulation of G_{M1} throughout the endocytic systems.

A study using a mouse model of G_{M1}-gangliosidosis showed that G_{M1} storage in the ER caused ER stress and altered calcium homeostasis (Sano *et al.* 2009). We have not examined calcium levels but confirmed that the levels of several ER chaperone proteins were up-regulated in neurons of our mouse model of G_{M1}-gangliosidosis (data not shown). It is possible that enhanced Trk-PLCγ signaling altered calcium homeostasis in the ER, as suggested in a previous study (Jia *et al.* 2007).

It has been reported that the major ubiquitin C-terminal hydrolase, UCHL1, was down-regulated in cells from patients with lysosomal storage disorders including G_{M1}-

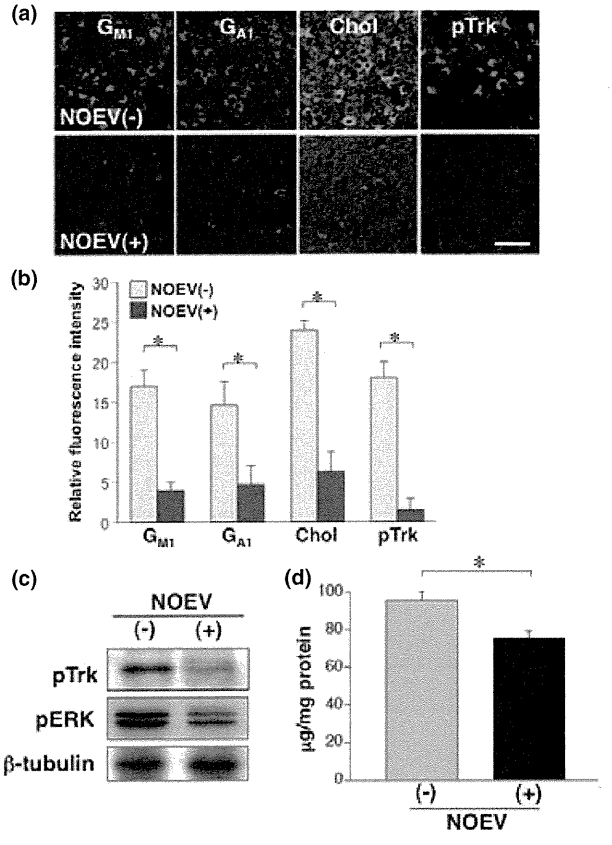

Fig. 7 NOEV ameliorates accumulation of pTrk in neurons of the R201C mouse brain. (a) Sections of cerebral cortex from R201C mice with or without administration of NOEV were stained with anti-G_{M1}, G_{A1}, pTrk and filipin, respectively. Images were obtained by confocal microscopy and representative images from three independent staining were shown. Scale bar, 50 μm. (b) Quantification of fluorescence images. Fluorescence signals were measured using Leica confocal software. Each column represents the mean ± SEM of 20 independent images. $^*p < 0.01$. (c) Immunoblotting of anti-pTrk, pERK and β-tubulin in lysates from R201C mice cortex. (d) Levels of total cholesterol in lysates from R201C mice cortex. $^*p < 0.01$.

gangliosidosis, as well as in the brain of a mouse model of Sandhoff disease (Bifsha *et al.* 2007). This phenotype could be mimicked with a cystein protease inhibitor E-64. Impairment of the ubiquitin-dependent protein degradation leads to aggregation of ubiquitin-labeled proteins, which is known as a common pathological mechanism of several neurodegenerative disorders such as Alzheimer's disease, Parkinson's disease and Huntington's disease (Rubinsztein 2006). The lysosomal storage of ubiquitin in the affected mice brains implicates that the ubiquitin pathway and the regulation of raft-mediated signaling may relate to a common neuropathological feature shared by different classes of lysosomal storage disorders (Vitner *et al.* 2010).

Accumulation of GSLs impairs autophagy in several lysosomal storage diseases (Settembre *et al.* 2008). In the previous study, we found storage of autophagy-related proteins, such as LC3 and beclin-1, which lead to mitochondrial dysfunction in β-gal−/− mouse brains. p62, an autophagosome-associated protein, was shown to interact with Trk protein to regulate neurotrophin signaling (Takamura *et al.* 2008). The increased levels of Trk proteins in anti-p62 IPs suggest impairment of autophagy that may cause the accumulation of Trk protein in β-gal−/− mouse brains.

In summary, we provided the evidence for lysosomal accumulation of Trk proteins and alteration of neurotrophin signaling in the G_{M1}-gangliosidosis mouse brains. Our findings suggest a potential therapeutic benefit of the suppression of Trk signaling in G_{M1}-gangliosidosis.

Acknowledgements

This work is supported by grants from Ministry of Education, Culture, Science, Sports and Technology of Japan (13680918, 14207106, 18390299, 20790728 and 21659257), Ministry of Health, Labour and Welfare of Japan (H17-Kokoro-019, H20-Kokoro-022 and a grant for Research for Intractable Diseases) and the Japan Health Sciences Foundation.

References

Bifsha P., Landry K., Ashmarina L. *et al.* (2007) Altered gene expression in cells from patients with lysosomal storage disorders suggests impairment of the ubiquitin pathway. *Cell Death Differ.* **14**, 511–523.

Brunetti-Pierri N. and Scaglia F. (2008) GM1 gangliosidosis: review of clinical, molecular, and therapeutic aspects. *Mol. Genet. Metab.* **94**, 391–396.

Choudhury A., Marks D. L., Proctor K. M., Gould G. W. and Pagano R. E. (2006) Regulation of caveolar endocytosis by syntaxin 6-dependent delivery of membrane components to the cell surface. *Nat. Cell Biol.* **8**, 317–328.

Duchemin A. M., Ren Q., Mo L., Neff N. H. and Hadjiconstantinou M. (2002) GM1 ganglioside induces phosphorylation and activation of Trk and Erk in brain. *J. Neurochem.* **81**, 696–707.

Duchemin A. M., Ren Q., Neff N. H. and Hadjiconstantinou M. (2008) GM1-induced activation of phosphatidylinositol 3-kinase: involvement of Trk receptors. *J. Neurochem.* **104**, 1466–1477.

Ferrari G., Anderson B. L., Stephens R. M., Kaplan D. R. and Greene L. A. (1995) Prevention of apoptotic neuronal death by GM1 ganglioside. Involvement of Trk neurotrophin receptors. *J. Biol. Chem.* **270**, 3074–3080.

Geetha T., Jiang J. and Wooten M. W. (2005) Lysine 63 polyubiquitination of the nerve growth factor receptor TrkA directs internalization and signaling. *Mol. Cell* **20**, 301–312.

Jia Y., Zhou J., Tai Y. and Wang Y. (2007) TRPC channels promote cerebellar granule neuron survival. *Nat. Neurosci.* **10**, 559–567.

Kiedrowski L., Czyz A., Baranauskas G., Li X. F. and Lytton J. (2004) Differential contribution of plasmalemmal Na/Ca exchange isoforms to sodium-dependent calcium influx and NMDA excitotoxicity in depolarized neurons. *J. Neurochem.* **90**, 117–128.

Manninen A., Verkade P., Le Lay S., Torkko J., Kasper M., Füllekrug J. and Simons K. (2005) Caveolin-1 is not essential for biosynthetic apical membrane transport. *Mol. Cell. Biol.* **25**, 10087–10096.

Matsuda J., Suzuki O., Oshima A. *et al.* (1997) Beta-galactosidase-deficient mouse as an animal model for GM1-gangliosidosis. *Glycoconj. J.* **14**, 729–736.

Matsuda J., Suzuki O., Oshima A. *et al.* (2003) Chemical chaperone therapy for brain pathology in G_{M1}-gangliosidosis. *Proc. Natl Acad. Sci. USA* **100**, 15912–15917.

Mutoh T., Tokuda A., Miyadai T., Hamaguchi M. and Fujiki N. (1995) Ganglioside GM1 binds to the Trk protein and regulates receptor function. *Proc. Natl Acad. Sci. USA* **92**, 5087–5091.

Nishio M., Fukumoto S., Furukawa K., Ichimura A., Miyazaki H., Kusunoki S., Urano T. and Furukawa K. (2004) Overexpressed GM1 suppresses nerve growth factor (NGF) signals by modulating the intracellular localization of NGF receptors and membrane fluidity in PC12 cells. *J. Biol. Chem.* **279**, 33368–33378.

Posse de Chaves E. and Sipione S. (2010) Sphingolipids and gangliosides of the nervous system in membrane function and dysfunction. *FEBS Lett.* **584**, 1748–1759.

Puri V., Watanabe R., Dominguez M., Sun X., Wheatley C. L., Marks D. L. and Pagano R. E. (1999) Cholesterol modulates membrane traffic along the endocytic pathway in sphingolipid-storage diseases. *Nat. Cell Biol.* **1**, 386–388.

Rabin S. J., Bachis A. and Mocchetti I. (2002) Gangliosides activate Trk receptors by inducing the release of neurotrophins. *J. Biol. Chem.* **277**, 49466–49472.

Rubinsztein D. C. (2006) The roles of intracellular protein-degradation pathways in neurodegeneration. *Nature* **443**, 780–786.

Sano R., Annunziata I., Patterson A., Moshiach S., Gomero E., Opferman J., Forte M. and d'Azzo A. (2009) GM1-ganglioside accumulation at the mitochondria-associated ER membranes links ER stress to Ca(2+)-dependent mitochondrial apoptosis. *Mol. Cell* **36**, 500–511.

Schönhöfer P. S. (1992) GM-1 ganglioside for spinal-cord injury. *N. Engl. J. Med.* **326**, 493.

Settembre C., Fraldi A., Rubinsztein D. C. and Ballabio A. (2008) Lysosomal storage diseases as disorders of autophagy. *Autophagy* **4**, 113–114.

Sugii S., Reid P. C., Ohgami N., Du H. and Chang T. Y. (2003) Distinct endosomal compartments in early trafficking of low density lipoprotein-derived cholesterol. *J. Biol. Chem.* **278**, 27180–27189.

Suzuki Y., Ichinomiya S., Kurosawa M. *et al.* (2007) Chemical chaperone therapy: clinical effect in murine G_{M1}-gangliosidosis. *Ann. Neurol.* **62**, 671–675.

Suzuki Y., Nanba E., Matsuda J., Higaki K. and Oshima A. (2008) β-Galactosidase deficiency (β-galactosidosis): G_{M1}-gangliosidosis and Morquio B disease, in *The Online Metabolic and Molecular Bases of Inherited Disease* (Valle D., Beaudet A. L., Vogelstein B., Kinzler K. W. and Antoanarakis S. F., eds), pp. 1–101. McGraw-Hill, New York, Chapter 151.

Takamura A., Higaki K., Kajimaki K., Otsuka S., Ninomiya H., Matsuda J., Ohno K., Suzuki Y. and Nanba E. (2008) Enhanced autophagy and mitochondrial aberrations in murine G_{M1}-gangliosidosis. *Biochem. Biophys. Res. Commun.* **367**, 616–622.

Vitner E. B., Platt F. M. and Futerman A. H. (2010) Common and uncommon pathogenic cascades in lysosomal storage diseases. *J. Biol. Chem.* **285**, 20423–20427.

Walkley S. U. and Vanier M. T. (2009) Secondary lipid accumulation in lysosomal disease. *Biochim. Biophys. Acta* **1793**, 726–736.

Wooten M. W., Geetha T., Babu J. R., Seibenhener M. L., Peng J., Cox N., Diaz-Meco M. T. and Moscat J. (2008) Essential role of sequestosome 1/p62 in regulating accumulation of Lys63-ubiquitinated proteins. *J. Biol. Chem.* **283**, 6783–6789.

Yu R. K., Bieberich E., Xia T. and Zeng G. (2004) Regulation of ganglioside biosynthesis in the nervous system. *J. Lipid Res.* **45**, 783–793.

RESEARCH ARTICLE

Human Mutation

OFFICIAL JOURNAL
HGVS
HUMAN GENOME VARIATION SOCIETY
www.hgvs.org

Chemical Chaperone Therapy: Chaperone Effect on Mutant Enzyme and Cellular Pathophysiology in β-Galactosidase Deficiency

Katsumi Higaki,[1]* Linjing Li,[1,2] Udin Bahrudin,[1,3,4] Soichiro Okuzawa,[5] Ayumi Takamuram,[1] Koichi Yamamoto,[1] Kaori Adachi1,[2] Rubigilda C. Paraguison,[1] Tomoko Takai,[1] Hiroki Ikehata,[1] Lika Tominaga,[1] Ichiro Hisatome,[3] Masami Iida,[6] Seiichiro Ogawa,[5] Junichiro Matsuda,[7] Haruaki Ninomiya,[8] Yasubumi Sakakibara,[5] Kousaku Ohno,[2] Yoshiyuki Suzuki,[9] and Eiji Nanba[1]

[1]Division of Functional Genomics, Research Center for Bioscience and Technology, Tottori University, Yonago, Japan; [2]Division of Child Neurology, Department of Neurological Science, Tottori University Faculty of Medicine, Yonago, Japan; [3]Division of Regenerative Medicine and Therapeutics, Institute of Regenerative Medicine and Biofunction, Tottori University Graduate School of Medical Science, Yonago, Japan; [4]Center of Biomedical Research, Medical Faculty Diponegoro University, Semarang, Indonesia; [5]Department of Biosciences and Informatics, Faculty of Science and Technology, Keio University, Kohoku-ku, Yokohama, Japan; [6]Central Research Laboratories, Seikagaku Corporation, Higashi-Yamato, Tokyo, Japan; [7]Laboratory of Animal Models for Human Diseases, National Institute of Biomedical Innovation, Ibaraki, Japan; [8]Department of Biomedical Regulation, School of Health Science, Tottori University, Faculty of Medicine, Yonago, Japan; [9]International University of Health and Welfare Graduate School, Otawara, Japan

Communicated by Hans R. Waterham

Received 10 September 2010; accepted revised manuscript 4 April 2011.
Published online 21 April 2011 in Wiley Online Library (www.wiley.com/humanmutation). DOI 10.1002/humu.21516

ABSTRACT: β-Galactosidase deficiency is a group of lysosomal lipid storage disorders with an autosomal recessive trait. It causes two clinically different diseases, G_{M1}-gangliosidosis and Morquio B disease. It is caused by heterogeneous mutations in the *GLB1* gene coding for the lysosomal acid β-galactosidase. We have previously reported the chaperone effect of *N*-octyl-4-epi-β-valienamine (NOEV) on mutant β-galactosidase proteins. In this study, we performed genotype analyses of patients with β-galactosidase deficiency and identified 46 mutation alleles including 9 novel mutations. We then examined the NOEV effect on mutant β-galactosidase proteins by using six strains of patient-derived skin fibroblast. We also performed mutagenesis to identify β-galactosidase mutants that were responsive to NOEV and found that 22 out of 94 mutants were responsive. Computational structural analysis revealed the mode of interaction between human β-galactosidase and NOEV. Moreover, we confirmed that NOEV reduced G_{M1} accumulation and ameliorated the impairments of lipid trafficking and protein degradation in β-galactosidase deficient cells. These results provided further evidence to NOEV as a promising chaperone compound for β-galactosidase deficiency.
Hum Mutat 32:843–852, 2011. © 2011 Wiley-Liss, Inc.

KEY WORDS: lysosomal storage disease; G_{M1}-gangliosidosis; *GLB1*; chaperone therapy; ubiquitin

Introduction

Acid β-galactosidase (GLB1 or β-gal; EC 3.2.1.23; MIM# 611458) is a lysosomal hydrolase that cleaves the terminal β-gal linkage in ganglioside G_{M1} and other glycoconjugates. Hereditary deficiency of lysosomal β-gal (or β-galactosidosis) is an autosomal recessive lipid storage disorder categorized into two clinical entities, G_{M1}-gangliosidosis (MIM# 230500) and Morquio B disease (MIM# 253010) [Brunetti-Pierri and Scaglia, 2008; Suzuki et al., 2008]. G_{M1}-ganglisidosis is a neurosomatic disease occurring mainly in early infancy or young adults. The infantile form is characterized by rapid progressive psychomotor deterioration, dysmorphism, and macular cherry-red spots. The late-infantile/juvenile form shows a milder clinical course without remarkable bone changes or visceromegaly. The adult or chronic form is uncommon with a more protracted clinical course. Morquio B disease is a rare bone disease without central nervous system involvement.

The human *GLB1* gene (MIM# 611458) encoding β-gal protein is composed of 16 exons and is mapped on 3p21.33 [Morreau et al., 1989; Oshima et al., 1988]. It expresses two alternatively spliced mRNAs, a major product for lysosomal β-gal and a minor product for elastin-binding protein. To date, more than 130 mutations have been reported in *GLB1* and common mutations have been found in some types of β-gal deficiency: I51T and R201H for adult G_{M1}-gangliosidosis, R201C for juvenile G_{M1}-gangliosidosis, and W273L for Morquio B disease [Brunetti-Pierri and Scaglia, 2008; Hofer et al., 2009, 2010; Suzuki et al., 2008].

The pathophysiological hallmark of this disease is a lysosomal accumulation of G_{M1}-ganglioside and its derivatives in neurons of the brain and a high amount of oligosaccharides in visceral organs

Additional Supporting Information may be found in the online version of this article.

*Correspondence to: Katsumi Higaki, Division of Functional Genomics, Research Center for Bioscience and Technology, Tottori University, 86 Nishi-cho, Yonago, 683-8503, Japan. E-mail: kh4060@med.tottori-u.ac.jp

Contract grant sponsor: Ministry of Education, Culture, Science, Sports and Technology of Japan; Contract grant numbers: 18390299; 20790728; 21659257; Contract grant sponsor: Ministry of Health, Labour and Welfare of Japan; Contract grant numbers: H10-No-006; H14-Kokoro-017; H17-Kokoro-019; H20-Kokoro-022, and a grant for Research for Intractable Diseases; Contract grant sponsor: The Japan Health Sciences Foundation.

and urine [Brunetti-Pierri and Scaglia, 2008; Suzuki et al., 2008]. Impaired autophagy and proteasome function has been shown to be related to pathogenesis of several lysosomal storage diseases (LSDs) including G_{M1}-gangliosidosis [Otomo et al., 2009; Settembre et al., 2008; Takamura et al., 2008]. Autophagic dysfunction leads to enhanced susceptibility to mitochondria-mediated apoptosis and to oxidative stress that activates inflammation processes [Luciani et al., 2010; Takamura et al., 2008].

At present, no specific therapy is available for patients with β-gal deficiency. Enzyme replacement therapy has been introduced for the treatment of Gaucher disease and other LSDs but is not applicable for the brain pathology of β-gal deficiency [Brady and Schiffmann, 2004]. Gene therapy has been shown to be of limited effect on bone and brain manifestations of β-gal deficiency [Takaura et al., 2005]. We have developed chemical chaperone (or pharmacological chaperone) therapy for LSDs [Fan et al., 1999; Iwasaki et al., 2006; Matsuda et al., 2003; Suzuki et al., 2007]. In this therapy, competitive enzyme inhibitors with a low molecular weight bind and stabilize the mutant protein in the endoplasmic reticulum (ER) and facilitate its transport to the lysosome [Parenti, 2010; Suzuki et al., 2009]. We have identified a novel valienaimine derivative, *N*-octyl-4-epi-β-valienamine (NOEV) as a potent chemical chaperone for mutant β-gal proteins [Matsuda et al., 2003; Ogawa et al., 2002]. Our initial study has shown that NOEV increased mutant β-gal activity in cultured fibroblasts and in the brain of G_{M1}-gangliosidosis mouse model [Iwasaki et al., 2006; Suzuki et al., 2007].

In this study, we have examined the chaperone effect of NOEV on human mutant β-gal proteins and cellular pathophysiology of affected cells.

Materials and Methods

Materials

Dulbecco's Modified Eagle's Medium (DMEM) and DMEM/F12 were obtained from Wako (Tokyo, Japan). Fetal bovine serum (FBS) was from HyClone Lab (Waltham, MA). Lipofectamine 2000 transfection reagent was from Invitrogen Corp. (Carlsbad, CA). NOEV was synthesized in Central Research Lab, Seikagaku Corp (Tokyo, Japan). Mouse monoclonal anti-ubiquitin (Ub; P4D1) and rabbit polyclonal anti-β-tubulin were purchased from Santa Cruz Biotech. Inc. (Santa Cruz, CA). Mouse monoclonal anti-G_{M1} (GMB16) was from Seikagaku Corp. (Tokyo, Japan). Rabbit polyclonal anti-p62/SQSTM1 (PM045) was from MBL Co. Ltd (Nagoya, Japan). Mouse monoclonal anti-golgin 97 (CDF4) and BODIPY FL C5-ceramide were from Molecular Probes (Invitrogen Corp., Carlsbad, CA). OptiPrep density gradient medium was from Axis-Shield (Oslo, Norway). 4-Methylumbelliferone (4-MU)-conjugated β-D-galactoside, α-D-galactoside, N-acetyl-β-D-glucosaminide and G_{M1} from bovine brain were from Sigma (St. Louis, MO).

Mutational Analysis

Total genome DNA was extracted from blood or harvested cultured primary skin fibroblasts from G_{M1}-gangliosidosis patients using a standard phenol-chloroform extraction procedure. DNA samples from healthy subjects were used as normal controls for heteroduplex formation. Polymerase chain reaction (PCR) amplification spanning from exons 1 to 16 of *GLB1* gene was performed using a number of primer sets (Supp. Table S1). All exons and flanking sequences of *GLB1* were screened for mutations by denaturing high-performance liquid chromatography (DHPLC, Transgenomic WAVE System, Omaha, NE) as described in Supp. Methods. Mutations were confirmed by direct sequencing (ABI 3130xl, Applied Biosystems, Foster City, CA) and were presented with a unified numbering system based on the sequence of GenBank entry NM_000404.2. The gene analysis of the patients was carried out according to the "Guidelines for Genetic Testing" by Genetic Medicine-Related Society in Japan.

Construction of Human β-Gal Expression Plasmids

Human β-gal cDNA (2.1 kb) was subcloned into a mammalian expression vector pCMV-Script (Stratagene, La Jolla, CA) [Oshima et al., 1988]. Mutations were introduced by Quick Change II site-directed mutagenesis (Stratagene) using oligonucleotide primers (Supp. Tables S2 and S3) following the manufacturer's protocol. All the 94 mutations (87 missense and 7 nonsense or frame shift mutations) were confirmed by sequencing. For transfection experiments, plasmid DNA was obtained using Plasmid DNA purification kit (Qiagen, Hilden, Germany).

Cell Culture, Transfection, and NOEV Treatment

Human skin fibroblasts from patients with β-gal deficiency were obtained in our laboratories or provided by colleagues at medical and scientific institutes (Supp. Methods). Human fibroblasts and mouse fibroblast cell lines from β-gal knockout (KO) mouse embryo [Matsuda et al., 2003] were cultured in DMEM supplemented with 10% FBS. Transfection was performed using Lipofectamine 2000 reagent following the manufacturer's protocol with minor modification. Briefly, β-gal-deficient mouse fibroblasts were prepared in 35-mm cultured dishes and transfected with a mixture of 2 μg of β-gal expression plasmids and 5 μl of Lipofectamine 2000 reagent. After 5 hr of incubation, cultured medium was replaced fresh medium with or without NOEV and cells were incubated for 48 hr. Mock pCMV-script DNA was used as a negative control. For human skin fibroblasts, cells from normal and six strains were cultured with or without NOEV and were incubated for 96 hr as described before [Iwasaki et al., 2006].

Lysosomal Enzyme Assay

Lysosomal enzyme activity in cell lysate was measured by using 4-MU substrates as described previously [Iwasaki et al., 2006]. Briefly, cells in 35-mm dishes were washed with phosphate-buffered saline (PBS) (4°C) and scraped into 100 μl 0.1% Triton X-100 in dH_2O. After centrifugation (6,000 rpm for 15 min at 4°C) to remove insoluble materials, 10 μl of lysates with 20 μl of the substrate solution in 0.1 M citrate buffer (pH 4.5) was incubated at 37°C for 30 min and the reaction was terminated by adding 0.2 M glycin-NaOH buffer (pH 10.7). The librated 4-MU was measured with a fluorescence plate reader (excitation 340 nm; emission 460 nm; Infinite F500, TECAN Japan, Kawasaki, Japan). Protein concentrations were determined using Protein Assay Rapid Kit (Wako, Tokyo, Japan) and enzyme activity was normalized by protein concentration.

Inhibition and Stabilization of β-Gal In Vitro

Cell lysates in 0.1% Triton X-100 in dH_2O from normal and patient (R201C/R201C) skin fibroblasts were used for in vitro analysis. For inhibition assay, lysates were mixed with 4-MU β-gal substrates in the absence or presence of increasing concentrations of NOEV. For heat stabilization, they were incubated in 0.1 M citrate buffer (pH 7) at 48°C for the time indicated, and then incubation was terminated by adding 2 volumes of 0.1 M citrate buffer (pH 4.5). The β-gal activity was measured as described above.

Protein Extraction, Subcellular Fractionation, and Western Blotting

Cells were lysed by sonication in 10 mM Tris-HCl (pH 7.4), 150 mM NaCl, 1 mM EDTA, 1 mM EGTA, 1% Triton X-100, and a protease inhibitor cocktail (Roche Diagnostics, Indianapolis, IN) and the supernatants were used as total extracts. For subcellular fractionation, extracted proteins were subjected to continuous gradient ultracentrifugation (90,000 × *g* for 20 hr at 4°C in SW 41Ti rotor) in OptiPrep gradient (Axis-Shield, Norway) as described previously [Sugii et al., 2003]. The top 20 fractions of the gradients were recovered and subjected to β-gal enzyme assay and Western blotting. Western blotting was performed as described previously [Otomo et al., 2009; Takamura et al., 2008]. Signals from horseradish peroxidase-conjugated secondary antibodies were visualized by ECL detection kit (GE Healthcare Bioscience, Piscataway, NJ) and images were obtained using LAS-4000 lumino image analyzer (Fujifilm, Tokyo, Japan).

Fluorescence Staining

All the procedures were carried out at room temperature as described previously [Otomo et al., 2009; Takamura et al., 2008]. Cultured cells were fixed with 4% paraformaldehyde in PBS for 30 min. They were permeabilized with 0.1% Triton X-100 in PBS for 15 min, blocked with 1% bovine serum albumin (BSA) for 1 hr, and incubated with primary antibodies for 1 hr. We used anti-G_{M1} at 1:50 dilution with 0.1% BSA/PBS. Bound antibodies were detected with Alexa-Fluor-conjugated secondary antibodies (diluted with 1:2,000 in 0.1% BSA/PBS) for 1 hr. Slides were coverslipped with Vectashild mounting media (Vector Laboratories, Burlingame, CA) and fluorescence images were obtained sequentially using a confocal laser microscopy (Leica TCS SP-2; Wetzler, Germany).

BODIPY-Cer Labeling

Prior to labeling, cells on the coverslip were incubated with 0.2 μM G_{M1} for 48 hr. They were then incubated with 5 μM BODIPY FL C5-Cer-BSA in Hank's-balanced salt solution for 30 min at 37°C, washed, and incubated in fresh medium for 30 min at 37°C. Then cells were fixed and stained with anti-golgin97. Fluorescence images were obtained using a confocal microscopy.

Molecular Simulation of Human β-Gal Structure and Its Interaction with NOEV

The three-dimensional structure of human β-gal enzyme protein was predicted using a sequence alignment of human and *Penicillium* sp. β-gal, and a homology modeling method 3D-JUDY [Suzuki et al., 2009]. The conformation of human β-gal and NOEV complex was computed by AUTODOCK4. The conformation was subjected to further structural optimization.

Primary Culture of Astrocytes from Mouse Brains

C57BL/6-based congenic strain KO mouse with β-gal deficiency and KO-Tg (knockout-transgenic) mice (I51T and R201C mice) that express human mutant I51T or R201C enzyme protein have been established and characterized by us [Matsuda et al., 1997, 2003]. All procedures were carried out according to the protocols approved by the committee for animal experiments in Tottori University. Primary astrocytes were cultured as described previously [Takamura et al., 2008]. Briefly, brains were removed from postnatal day 4 mice under anesthesia. The cerebral cortex was dissociated and cells were seeded on plastic dishes in DMEM/F12 supplemented with 15% FBS. They were cultured for 7 days, trypsinized, and seeded on dishes with DMEM-F12 with 10% FBS. They were confirmed to be GFAP-positive astrocytes at 3 weeks (data not shown).

Results

Mutation Analysis of G_{M1}-Gangliosidosis Patients

The DHPLC and sequence analyses identified 46 mutation alleles including 9 novel mutations in 26 patients with G_{M1}-gangliosidosis (Supp. Fig. S1 and Table 1).

Characterization of NOEV Effects in Cell Lysate from Human Skin Fibroblasts

Chemical structure of NOEV is shown in Figrue 1A [Ogawa et al., 2002]. NOEV inhibited β-gal activity in cell lysates of cultured human skin fibroblasts at pH 5 (Fig. 1B). It was effective both in cells from normal and R201C/R201C patient with IC_{50} values of 0.125 and 0.132 μM, respectively, at pH 5 (Fig. 1B). NOEV has no effects on α-gal or β-hexosaminidase (β-hex) under the same conditions. To evaluate in vitro NOEV effects on enzyme stabilization, lysates were preincubated with increasing concentrations of NOEV and were subjected to heat inactivation (48°C) at pH 7.0. In the absence of NOEV, the activities of normal and R201C β-gal decreased to 11 and 7% after a 30-min incubation, respectively. NOEV ameliorated these decreases in a dose-dependent manner (Fig. 1C).

Chaperone Effects of NOEV in Cultured Human Skin Fibroblasts

To evaluate the chemical chaperone effect of NOEV in cultured human skin fibroblasts, cells were cultured in the medium with increasing concentrations of NOEV for 96 hr, and the β-gal enzyme activity in cell lysates was determined. In the six lines with β-gal deficiency, we found significant chaperone effects of NOEV in three lines, which contained β-gal mutations of G190D/G190D (patient #18), R201C/R201C and R457Q/R457Q. NOEV had no effects in cells with β-gal mutations of I51T/I51T, I51T/Y316C (patient #24) and G438E/G438E (Fig. 2A). To examine whether NOEV enhanced trafficking of the mutant enzyme protein to the lysosomes, we performed the subcellular fractionation experiments. Immunoblot analyses of each fraction showed the localization of the ER marker calnexin in fractions #1–4 and that of the lysosome marker lamp-2 in fractions #12–16, and the localization of these markers were indistinguishable between control and R201C/R201C cells (data not shown). In fractions from control cells, the β-gal activity was recovered mainly in fractions #12–17 (data not shown). The same analysis of R201C/R201C cell fractions showed broad distribution of β-gal activity with peaks at #1 and #15 (Fig. 2B). NOEV treatment of R201C/R201C cells increased the activity up to four folds in #12–16, which suggested increased transport of mutant protein to the late endosomes/lysosomes in cells treated with NOEV.

Intracellular Trafficking of BODIPY-Ceramide

We also examined trafficking of fluorescence-labeled ceramide. BODIPY-labeled ceramide was internalized and subsequently

Table 1. Mutations in *GLB1* Gene Causing G_{M1}-Gangliosidosis

Patient	Nucleotide change[a]	Predicted aa change	Clinical phenotype	Ethnic origin	References
1	c.1438A>G	p.M480V	Inf G_{M1}	Japanese	This study
	c.1445G>A	p.R482H			Mosna et al. [1992]
2	c.442C>T	p.R148C	Inf G_{M1}	Japanese	Nishimoto et al. [1991]
	?	?			(−)
3	c.622C>T	p.R208C	Inf G_{M1}	Japanese	Boustany et al. [1993]
	c.622C>T	p.R208C			Boustany et al. [1993]
4	c.176G>A	p.R59H	Inf G_{M1}	Japanese	Silva et al. [1999]
	c.996C>G	p.D332E			Hofer et al. [2009]
5	c.1445G>A	p.R482H	Inf G_{M1}	Japanese	Mosna et al. [1992]
	c.1646C>T	p.P549L			Santamaria et al. [2007]
6	c.276−277insG	p.P93AfsX7	Inf G_{M1}	Japanese	This study
	?	?			(−)
7	c.542T>A	p.I181K	Inf G_{M1}	Turkish	Hofer et al. [2010]
	c.542T>A	p.I181K			Hofer et al. [2010]
8	c.601C>T	p.R201C	Adul G_{M1}	unknown	Oshima et al. [1991]
	c.602G>A	p.R201H			Oshima et al. [1995]
9	c.161G>T	p.S54I	Inf G_{M1}	unknown	This study
	?	?			(−)
10	c.175C>T	p.R59C	Adul G_{M1}	unknown	Caciotti et al. [2005]
	c.245C>T	p.T82M			Chakraborty et al. [1994]
11	c.601C>T	p.R201C	Adul G_{M1}	Japanese	Oshima et al. [1991]
	c.1259C>A	p.T420K			Santamaria et al. [2006]
12	c.145C>T	p.R49C	Inf G_{M1}	Estonian	Nishimoto et al. [1991]
	c.391G>A	p.E131K			This study
13	c.601C>T	p.R201C	Inf G_{M1}	Estonian	Oshima et al. [1991]
	c.808T>G	p.Y270D			Paschke et al. [2001]
14	c.1343A>T	p.D448V	Inf G_{M1}	Japanese	Hofer et al. [2010]
	c.1746G>A	p.W582X			This study
15	c.176G>A	p.R59H	Inf G_{M1}	Japanese	Silva et al. [1999]
	c.1820T>C	p.L608P			This study
16	c.436_438delCTT	p.L146del	Inf G_{M1}	Japanese	This study
	?	?			(−)
17	c.176G>A	p.R59H	Inf G_{M1}	UAE	Silva et al. [1999]
	c.176G>A	p.R59H			Silva et al. [1999]
18	c.569G>A	p.G190D	Inf G_{M1}	Turkish	Hofer et al. [2009]
	c.569G>A	p.G190D			Hofer et al. [2009]
19	c.276G>A	p.W92X	Inf G_{M1}	Indian	This study
	c.276G>A	p.W92X			This study
20	c.75+2_3insT		Inf G_{M1}	Belgian	Chakraborty et al. [1994]
	c.75+2_3insT				Chakraborty et al. [1994]
21	c.569G>A	p.G190D	Inf G_{M1}	Turkish	Hofer et al. [2009]
	c.569G>A	p.G190D			Hofer et al. [2009]
22	c.569G>A	p.G190D	Inf G_{M1}	Turkish	Hofer et al. [2009]
	c.569G>A	p.G190D			Hofer et al. [2009]
23	c.841C>T	p.H281Y	Inf G_{M1}	Russia	Paschke et al. [2001]
	?	?			(−)
24	c.152T>C	p.I51T	Adul G_{M1}	Japanese	Oshima et al. [1991]
	c.947A>G	p.Y316C			Oshima et al. [1991]
25	c.428_429insA	p.S144VfsX42	Inf G_{M1}	British	This study
	?	?			(−)
26	c.602G>A	p.R201H	Adul G_{M1}	Belgian	Oshima et al. [1995]
	c.1441G>T	p.G481X			Santamaria et al. [2006]

[a]The numbering for the nucleotide changes are based on cDNA sequence with GenBank entry NM_000404.2. with +1 corresponding to the A of ATG translation initiation codon in the reference sequence.

transported to the Golgi complex in normal cells. In consistence with the previous reports [Marks and Pagano, 2002; Puri et al., 1999], it was localized to the perinuclear punctuates in affected cells when cells were cultured with G_{M1} (Fig. 2C). NOEV treatment restored the transport of BODIPY-ceramide to the Golgi apparatus in G190D/G190D (patient #18), R201C/R201C and R457Q/R457Q cells, but not in I51T/I51T and G438E/G438E cells.

Screening of NOEV Effects on Human Mutant β-Gal Proteins

We next screened NOEV effects on 94 different β-gal mutants (Supp. Table S2) by using transient expression in β-gal-deficient fibroblasts. After trasfection, cells were incubated with increasing concentrations of NOEV for 48 hr and the β-gal in cell lysates was determined. 22 missense mutants responded to NOEV (Fig. 3 and Supp. Fig. S2). The maximum response was obtained at 2 μM in most of the responsive mutants except for 7 (L173P, N318H, D332E, Y444C, R457Q, R590C, and R590H). Several mutants (D214Y, W273R, N318H, Y347C, Y444C, and R590H) showed high residual activities (more than 10% of normal activity). The tertiary structure of human β-gal protein was predicted by homology modeling using *Penicillium* sp. β-gal as a template and the interaction between β-gal protein and NOEV was predicted by AUTODOCK4 [Jo et al., 2010; Suzuki et al., 2009]. The mutations responsive to NOEV were localized throughout the various

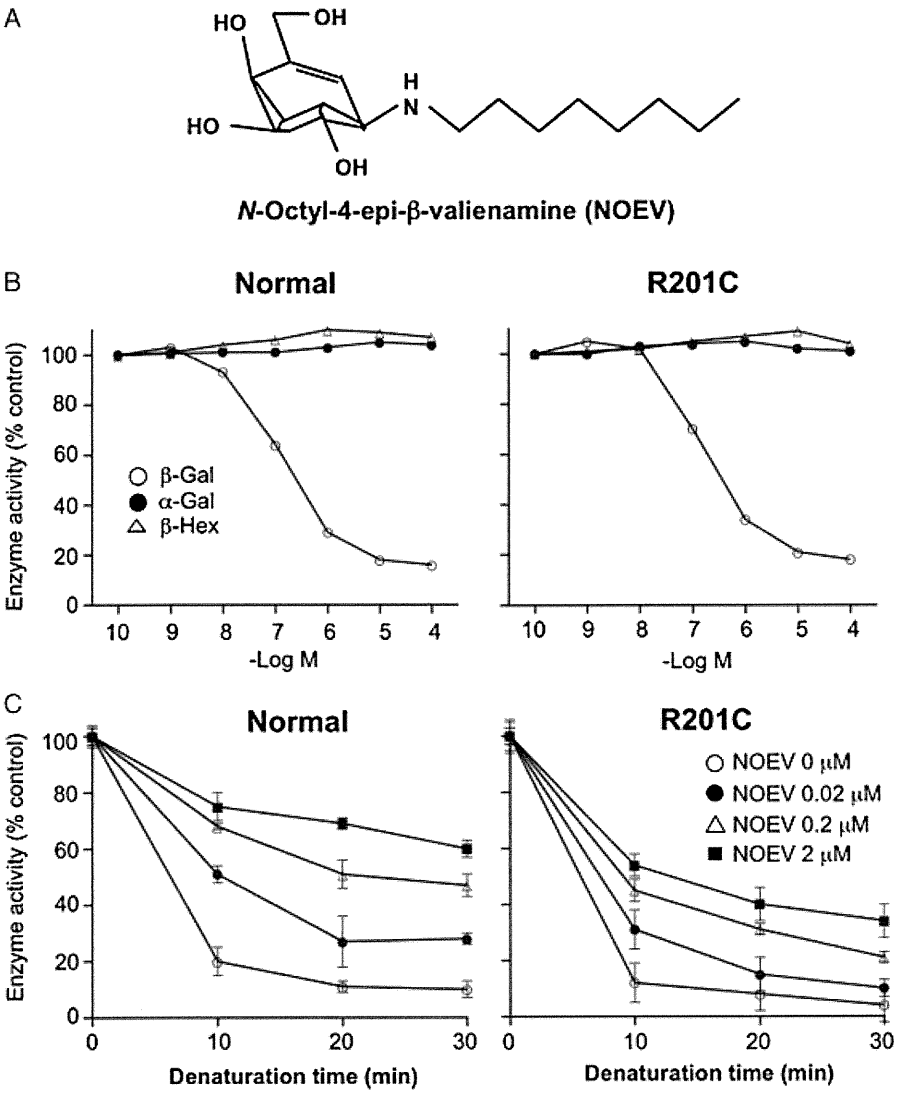

Figure 1. NOEV binds to and stabilizes human β-galactosidase proteins in vitro. **A:** Structure of NOEV. **B:** Enzyme activities in cell lysates from normal and patient fibroblast with R201C/R201C mutations were determined after incubation with or without NOEV. **C:** Cell lysates were incubated at pH 7.0 and 48°C for the indicated time and the β-gal activity was measured. Each point represents means of triplicates obtained in at least three independent experiments. Values were expressed as relative to the activity in the absence of NOEV as 100%.

protein regions including triosephosphateisomerase (TIM) motif (Fig. 4) [Kang and Stevens, 2009].

NOEV Reduced G_{M1} Accumulation and Protein Ubiquitination in Primary Cultured Mouse Astrocytes Expressing R201C β-Gal

G_{M1} is enriched in the plasma membrane lipid microdomain (also known as lipid rafts), particularly in neurons and astrocytes. Because fibroblasts do not accumulate G_{M1} to the same extent as neuronal cells, we next investigated NOEV effects using astrocytes isolated from mouse brain. The activity of β-gal was undetectable in β-gal$^{-/-}$ astrocytes, but some activities were detected in R201C and I51T cells (Fig. 5A). Immunostaining with anti-G_{M1} showed lysosomal G_{M1} accumulation in these cells, whereas no such staining was detected in wild-type (wt) astrocytes (Fig. 5B). Treatment with 0.2 μM NOEV increased the enzyme activity and reduced G_{M1} accumulation in R201C cells, indicating the effectiveness of NOEV as shown in fibroblasts. Although NOEV significantly reduced β-gal activity in the wt cells, no such effect was observed in β-gal$^{-/-}$ and I51T cells.

We and others have proposed that impairments of the protein degradation pathways play an important role in neurodegeneration of several lysosomal storage diseases [Otomo et al., 2009; Settembre et al., 2008; Takamura et al., 2008]. p62, also known as sequestosome-1 is an adaptor protein, initially isolated as an interacting partner of atypical proteins kinase C [Sanchez et al., 1998]. Recent studies suggest that p62 is a ubiquitin- and LC3-binding protein, that regulates the formation of protein aggregates and is removed by autophagy [Ichimura et al., 2008; Komatsu et al., 2007]. Immunofluorescence analysis in astrocytes revealed that p62 accumulated in β-gal$^{-/-}$ and R201C but not in wt cells, and NOEV significantly reduced p62 accumulation in R201C cells (Fig. 5C). No change was observed in p62 protein levels in wt and β-gal$^{-/-}$ cells after NOEV treatment. These results were confirmed in immunoblot analysis of cell lysates from astrocytes (Fig. 5D).